

~~RESTRICTED~~

Copy 236  
RM E9L02

NACA RM E9L02

E 9 L 02

0069269

TECH LIBRARY KAFB, NM

NACA

# RESEARCH MEMORANDUM

ALTITUDE-WIND-TUNNEL INVESTIGATION OF COMBUSTION-CHAMBER  
PERFORMANCE ON J47 TURBOJET ENGINE

By Carl E. Campbell

Lewis Flight Propulsion Laboratory  
Cleveland, Ohio

AFMDC  
TECHNICAL LIBRARY  
AFL 2811

CLASSIFIED DOCUMENT

This document contains classified information affecting the National Defense of the United States within the meaning of the Espionage Act, USC-5631 and 52. Its transmission or the revelation of its contents in any manner to an unauthorized person is prohibited by law.

Information so classified may be imparted only to persons in the military and naval services of the United States, appropriate civilian officers and employees of the Federal Government who have a legitimate interest therein, and to United States citizens of known loyalty and discretion who of necessity must be informed thereof.

NATIONAL ADVISORY COMMITTEE  
FOR AERONAUTICS

WASHINGTON  
December 15, 1950

~~RESTRICTED~~

6591

Declassified by Authority of LARC Security  
Classification office (SC) letter dated 14 June 83.  
Mason Foxman

319. 98/13

National Aeronautics and  
Space Administration

Langley Research Center  
Hampton, Virginia  
23665

NASA

Reply to AIN of 139A

JUN 1 6 1983

TO: Distribution  
FROM: 180A/Security Classification Officer  
SUBJECT: Authority to Declassify NACA/NASA Documents Dated Prior to  
January 1, 1960

*(informal, correspondence)*  
Effective this date, all material classified by this Center prior to  
January 1, 1960, is declassified. This action does not include material  
derivatively classified at the Center upon instructions from other Agencies.

Immediate re-marking is not required; however, until material is re-marked by  
lining through the classification and annotating with the following statement,  
it must continue to be protected as if classified:

"Declassified by authority of LARC Security Classification Officer (SCO)  
letter dated June 16, 1983," and the signature of person performing the  
re-marking.

If re-marking a large amount of material is desirable, but unduly burdensome,  
custodians may follow the instructions contained in NHB 1640.4, subpart F,  
section 1203.604, paragraph (h).

This declassification action complements earlier actions by the National  
Archives and Records Service (NARS) and by the NASA Security Classification  
Officer (SCO). In Declassification Review Program 807008, NARS declassified  
the Center's "Research Authorization" files, which contain reports, Research  
Authorizations, correspondence, photographs, and other documentation.  
Earlier, in a 1971 letter, the NASA SCO declassified all NACA/NASA formal  
series documents with the exception of the following reports, which must  
remain classified:

Document No.

E-51A30  
E-53G20  
E-53G21  
E-53K18  
SL-54J21a  
E-55C16  
E-56A23a

First Author

Hagey  
Francisco  
Johnson  
Spooner  
Westphal  
Fox  
Himmel

JUN 2 3 1983

If you have any questions concerning this matter, please call Mr. William L. Simkins at extension 3281.

*Jess G. Ross*  
 Jess G. Ross  
 2898

Distributions:  
 SDL 031

cc:  
 NASA Scientific and Technical  
 Information Facility  
 P.O. Box 8757  
 BWI Airport, MD 21240

NASA--NIS-5/Security  
 180A/RIAD  
 139A/TUSAO

*6-15-83*  
 139A/WLSimkins:elf 06/15/83 (3281)

*6-15-83*  
 139A/JS

BLOC 1194

MAIL STOP 188

HEADS OF ORGANIZATIONS  
 JANE S. HESS



0069269

NACA RM E9102

~~RESTRICTED~~

## NATIONAL ADVISORY COMMITTEE FOR AERONAUTICS

RESEARCH MEMORANDUM

## ALTITUDE-WIND-TUNNEL INVESTIGATION OF COMBUSTION-CHAMBER

## PERFORMANCE ON J47 TURBOJET ENGINE

By Carl E. Campbell

## SUMMARY

Combustion-chamber performance characteristics of the J47 turbojet engine were determined during an investigation of the complete engine in the NACA Lewis altitude wind tunnel. The data presented were obtained over a range of engine speeds at simulated altitudes from 5000 to 50,000 feet, flight Mach numbers from 0.21 to 0.97, and exhaust-nozzle-outlet areas from 280 to 342 square inches. The combustion-chamber performance characteristics are presented as functions of the engine speed corrected to NACA standard sea-level static conditions.

At a corrected engine speed of 7900 rpm, the combustion efficiency with the standard exhaust nozzle varied from 0.95 to 0.99 over the range of altitudes and flight Mach numbers investigated. Combustion efficiency was lowered by increasing the exhaust-nozzle-outlet area. The combustion-chamber over-all total-pressure-loss ratio decreased with an increase in altitude. Increasing the flight Mach number increased the over-all total-pressure-loss ratio at medium and low corrected engine speeds, but in the region of maximum engine speed the effect of flight Mach number was negligible. Changing the exhaust-nozzle-outlet area from 280 to 342 square inches had no appreciable effect on the over-all total-pressure-loss ratio. The fractional loss in engine cycle efficiency due to combustion-chamber total-pressure losses was not affected by changes of altitude and flight Mach number at high corrected engine speeds. Increasing the exhaust-nozzle-outlet area increased the fractional loss in engine cycle efficiency over the entire range of corrected engine speeds. The fractional loss in cycle efficiency due to the combustion-chamber pressure losses was approximately 0.04 with the standard exhaust nozzle at maximum engine speed.

~~RESTRICTED~~

## INTRODUCTION

An investigation to determine the performance and operational characteristics of a J47 turbojet engine and its components has been conducted in the NACA Lewis altitude wind tunnel over a wide range of simulated-flight conditions. Performance characteristics of the combustion chamber are evaluated herein. Over-all engine performance characteristics are presented in reference 1. Compressor and turbine performance characteristics are presented in references 2 and 3, respectively.

The manner of heat release and the flow characteristics of the combustion chamber influence the over-all performance of the turbojet engine. If combustion is incomplete, burning may occur through the turbine and raise the turbine-blade temperature above safe limits. The loss in total pressure through the combustion chamber reduces the cycle efficiency and also results in a slight reduction in the mass flow of air through the engine (reference 4).

Results are presented to indicate the effect of altitude, flight Mach number, and exhaust-nozzle-outlet area on the combustion efficiency, the losses in total pressure occurring in the combustion chamber, and the fractional loss in engine cycle efficiency resulting from combustion-chamber pressure losses. The engine cycle efficiency is also presented. These results are shown graphically as a function of corrected engine speed and in tabular form.

## ENGINE AND INSTALLATION

The J47 turbojet engine used in this investigation has a static sea-level thrust rating of 5000 pounds at an engine speed of 7900 rpm and a turbine-outlet temperature of 1275° F. At this rating, the air flow is 94 pounds per second and the fuel consumption is approximately 5250 pounds per hour. The principal components of this engine are a 12-stage axial-flow compressor, eight cylindrical through-flow combustion chambers, a single-stage impulse turbine, a tail pipe, and an exhaust nozzle. The exhaust nozzle, designated as standard, gave limiting turbine-outlet temperature at rated speed and static conditions at an altitude of 5000 feet, and had an outlet area of 280 square inches. In order to extend the range of investigation of the engine, oversize exhaust nozzles with outlet areas of 302 and 342 square inches were also used.

1218 The engine was mounted on a wing section that spanned the 20-foot-diameter test section of the altitude wind tunnel (fig. 1). Engine-inlet conditions corresponding to the simulated flight conditions were obtained by introducing dry refrigerated air from the tunnel make-up air system through a duct to the engine inlet. Air was throttled from approximately sea-level pressure to the desired pressure at the engine inlet, while the static pressure in the tunnel test section was maintained to correspond to the desired altitude.

Pressure and temperature instrumentation was installed at several stations through the engine (fig. 2). The combustion-chamber performance is chiefly determined by instrumentation at the compressor outlet (station 3), the turbine inlet (station 4), the turbine outlet (station 6), and the exhaust-nozzle outlet (station 7). Instrumentation at these stations is shown in detail in figure 3.

#### DESCRIPTION OF COMBUSTION CHAMBER

The eight combustion chambers are the cylindrical through-flow type, as shown in the cross-sectional drawing of the engine in figure 2. Each combustion chamber is fitted with inlet and outlet ducts leading from the compressor outlet and to the turbine inlet, respectively. The combustion zone in each chamber is separated from the outer shell by a liner (fig. 4). Louvres in the upstream face of the liner dome admit primary air to the combustion zone. Secondary air enters the combustion zone through eight equally-spaced longitudinal rows of 3/4-inch diameter holes and a series of louvres on the liner surface. The cross-sectional area of the combustion zone in each chamber varies from approximately 0.282 square foot at the plane of the first series of secondary air holes to 0.328 square foot at the plane of the final series of holes.

Each combustion chamber is equipped with a duplex fuel nozzle having a small-slot and large-slot element, and the nozzle extends into the combustion zone through a hole in the center of the liner dome. At the low fuel flows that accompany the starting process and operation at high altitude, all the fuel flows through the small slots, which are designed to provide a good spray pattern at fuel pressures down to approximately 20 pounds per square inch. As the fuel-flow requirements of the engine increase, a portion of the fuel, as determined by the automatic flow-divider mechanism, is injected through the large-slot element of the nozzle.

The ignition system consists of two high-voltage vibrator coils and two spark plugs. The vibrator coils are mounted on the upper half of the compressor casing and the spark plugs are installed in diametrically opposite combustion chambers. The spark-plug electrodes are located within the design spray cone of the fuel nozzles. Ignition is provided to the remaining combustion chambers through inter-connecting cross-fire tubes.

1218

### PROCEDURE

The investigation extended over a range of simulated altitudes from 5000 to 50,000 feet and simulated-flight Mach numbers from 0.21 to 0.97. Two additional exhaust nozzles with outlet areas of 302 and 342 square inches were used on the engine as well as the standard-size exhaust nozzle, which had an outlet area of 280 square inches. Engine inlet-air temperatures were maintained at NACA standard values for simulated altitudes up to 25,000 feet. At pressure altitudes above 25,000 feet, the inlet-air temperature was approximately  $-20^{\circ}\text{F}$ , which was the minimum temperature that could be obtained. Total pressure at the engine inlet was regulated to correspond to the pressure that would exist with complete free-stream ram-pressure recovery at each flight condition.

Air-flow calculations were made from pressure and temperature measurements obtained at the cowl inlet. Fuel flow was measured with a rotameter. The symbols and the methods of calculation used to determine the combustion-chamber performance from the pressure and temperature measurements are given in the appendix.

### RESULTS AND DISCUSSION

#### Combustion Efficiency

In order to indicate the effect of altitude on combustion efficiency, results obtained with the standard exhaust nozzle are presented in figure 5 for a range of altitudes between 5000 and 50,000 feet at flight Mach numbers of 0.21 and 0.52. The effect of altitude on combustion efficiency was similar at both flight Mach numbers. At altitudes below 25,000 feet, the combustion efficiency reached peak values at corrected engine speeds between 5000 and 6000 rpm and then decreased to a value of 0.95 at a corrected engine speed of 7900 rpm. The reason for this decrease in combustion efficiency in the high engine-speed region is not clear. At altitudes above 25,000 feet, the combustion efficiency increased steadily with engine speed to values between 0.97 and 0.99 at a corrected engine speed of 7900 rpm. The values of combustion efficiency presented in this report are accurate to approximately  $\pm 0.04$ .

The effect of flight Mach number on the combustion efficiency with the standard exhaust nozzle is shown for altitudes of 25,000 and 35,000 feet in figure 6. The trends were in general the same at both altitudes with the combustion efficiency reaching values from 0.97 to 0.99 at a corrected engine speed of 7900 rpm. At any corrected engine speed above 5000 rpm, the variation of combustion efficiency with changes in flight Mach number from 0.21 to 0.97 was less than 0.03.

The effect of exhaust-nozzle-outlet area on combustion efficiency at a flight Mach number of 0.21 and at simulated altitudes of 5000 and 25,000 feet is shown in figure 7. At an altitude of 5000 feet, the variation of combustion efficiency with engine speed was similar with each of the three exhaust nozzles. At this altitude, increasing the exhaust-nozzle-outlet area from 280 to 342 square inches reduced the peak efficiency from 0.99 to 0.97 and reduced the efficiency at a corrected engine speed of 7900 rpm from 0.95 to 0.93. At an altitude of 25,000 feet, the decrease in combustion efficiency with increased exhaust-nozzle-outlet area was more pronounced than at an altitude of 5000 feet, which was probably due to the lower combustion-chamber inlet pressure at 25,000 feet altitude. At this altitude at a corrected engine speed of 7900 rpm, the combustion efficiency decreased from 0.97 to 0.92 as the exhaust-nozzle area was increased from 280 to 342 square inches.

#### PRESSURE LOSSES

Measured values of over-all total-pressure-loss ratio were obtained directly from the pressure instrumentation at stations 3 and 4. Calculated values of over-all total-pressure-loss ratio were obtained by adding the friction and momentum pressure-loss ratios determined by the method explained in reference 5. Friction pressure losses were calculated by means of equation (7c) in the appendix with a value of the friction factor  $K$  determined from windmilling data. Momentum pressure losses were determined from the pressure-loss chart of reference 5 and the combustion-chamber equivalent area  $A_p$ . The measured and calculated values of the over-all total-pressure-loss ratios were reasonably similar in magnitude and trend throughout the data investigated.

The effect of altitude on over-all, friction, and momentum pressure-loss ratios with the standard exhaust nozzle at a flight Mach number of 0.21 is shown in figure 8. In general, an increase in altitude resulted in a decrease in the over-all total-pressure-loss ratio  $\Delta P_T/P_3$ . The friction and momentum pressure-loss data show that the reduction in  $\Delta P_T/P_3$  was due entirely to decreases



in friction pressure loss as the altitude was increased. The momentum pressure-loss ratio  $\Delta P_M/P_3$  was unaffected by changes in altitude over the entire range of corrected engine speeds. At the design speed of 7900 rpm, the maximum value of  $\Delta P_T/P_3$  obtained with the standard exhaust nozzle at a flight Mach number of 0.21 was approximately 0.04.

The effect of flight Mach number on the pressure-loss ratios with the standard exhaust nozzle at an altitude of 25,000 feet is shown in figure 9. An increase in flight Mach number resulted in a large increase in the over-all total-pressure-loss ratio at low corrected engine speeds because the increase in  $\Delta P_T/P_3$  was greater than the decrease in  $\Delta P_M/P_3$  as the flight Mach number was increased. At a corrected engine speed of 7900 rpm, the over-all total-pressure-loss ratio obtained with the standard exhaust nozzle was approximately 0.04 for all flight Mach numbers at a simulated altitude of 25,000 feet.

The effect of exhaust-nozzle-outlet area on the combustion-chamber pressure-loss ratios at an altitude of 5000 feet and a flight Mach number of 0.21 is shown in figure 10. The over-all total-pressure-loss ratio was affected only slightly by the increase in exhaust-nozzle-outlet area. The friction pressure-loss ratio increased and the momentum pressure-loss ratio decreased as the nozzle area was increased, with the resultant small effect on  $\Delta P_T/P_3$ .

#### CYCLE-EFFICIENCY LOSSES

The effect of altitude on the engine cycle efficiency  $\eta$  and the fractional loss in engine cycle efficiency  $\Delta\eta/\eta$  due to combustion-chamber pressure losses is shown in figure 11 for the standard exhaust nozzle and a flight Mach number of 0.21. The value of  $\Delta\eta/\eta$  decreased with an increase in corrected engine speed over the entire operating range. At corrected engine speeds above 5500 rpm,  $\Delta\eta/\eta$  did not vary with altitude. The value of  $\Delta\eta/\eta$  at the design corrected engine speed (7900 rpm) was about 0.04.

The effect of flight Mach number on  $\eta$  and  $\Delta\eta/\eta$  at an altitude of 25,000 feet with the standard exhaust nozzle is shown in figure 12. The fractional loss in cycle efficiency increased considerably with flight Mach number at corrected engine speeds below 6000 rpm. At the low corrected engine speeds, the value

of  $\Delta\eta/\eta$  was more than half of the efficiency obtained. In the region of the design corrected engine speed (7900 rpm), however, the value of  $\Delta\eta/\eta$  was about 0.04 and was unaffected by changes in flight Mach number.

The effect of exhaust-nozzle-outlet area on  $\eta$  and  $\Delta\eta/\eta$  at an altitude of 5000 feet and a flight Mach number of 0.21 is shown in figure 13. Increasing the exhaust-nozzle-outlet area increased the value of  $\Delta\eta/\eta$  over the entire operating range, particularly at the low corrected engine speeds. At the corrected engine speed of 7900 rpm, the values of  $\Delta\eta/\eta$  obtained with exhaust-nozzle-outlet areas of 280, 302, and 342 square inches were 0.04, 0.06, and 0.10, respectively.

#### SUMMARY OF RESULTS

From an altitude-wind-tunnel investigation of a J47 turbojet engine, the following combustion-chamber performance characteristics were obtained:

1. At a corrected engine speed of 7900 rpm, the combustion efficiency with the standard exhaust nozzle varied from 0.95 to 0.99 over the range of altitudes and flight Mach numbers investigated. Combustion efficiency was lowered by increasing the exhaust-nozzle outlet area.

2. The combustion-chamber over-all total-pressure-loss ratio  $\Delta P_T/P_3$  decreased with an increase in altitude. Increasing the flight Mach number increased the value of  $\Delta P_T/P_3$  at medium and low corrected engine speeds, but in the region of maximum engine speed the effect of flight Mach number was negligible. Changing the exhaust-nozzle outlet area from 280 to 342 square inches had no appreciable effect on  $\Delta P_T/P_3$ . At the design engine speed of 7900 rpm, the maximum value of  $\Delta P_T/P_3$  obtained with the standard exhaust nozzle was approximately 0.04 for all flight conditions investigated.

3. The fractional loss in engine cycle efficiency  $\Delta\eta/\eta$  due to combustion-chamber total-pressure losses was unaffected by changes in altitude and flight Mach number at high corrected engine speeds. At corrected engine speeds below 6000 rpm, an increase in flight Mach number increased  $\Delta\eta/\eta$  considerably.

Increasing the exhaust-nozzle-outlet area increased the value of  $\Delta\eta/\eta$  over the entire operating range. At the design engine speed of 7900 rpm, the fractional loss in cycle efficiency with the standard exhaust nozzle was approximately 0.04 at all flight conditions.

Lewis Flight Propulsion Laboratory,  
National Advisory Committee for Aeronautics,  
Cleveland, Ohio.

1218

## APPENDIX-CALCULATIONS

## Symbols

The following symbols are used in this report:

A	cross-sectional area, sq ft
$A_b$	area of equivalent combustion chamber of constant cross section, sq ft
$c_p$	specific heat at constant pressure, Btu/(lb)(°R)
f/a	fuel-air ratio in combustion chamber
g	acceleration due to gravity, 32.17 ft/sec <sup>2</sup>
H	total enthalpy, Btu/lb
J	mechanical equivalent of heat, 778 ft-lb/Btu
K	combustion-chamber friction pressure-loss factor
N	rotational speed of engine, rpm
P	total pressure, lb/sq ft absolute
$\Delta P_F$	friction pressure loss; loss in total pressure across combustion chamber due to friction, lb/sq ft
$\Delta P_M$	momentum pressure loss; loss in total pressure across combustion chamber due to heat addition, lb/sq ft
$\Delta P_T$	over-all total-pressure loss; loss in total pressure across combustion chamber due to friction and heat addition, lb/sq ft
p	static pressure, lb/sq ft absolute
R	gas constant, 53.3 ft-lb/(lb)(°R)
T	total temperature, °R
$T_i$	indicated temperature, °R
t	static temperature, °R
$W_a$	air flow, lb/sec

$W_f$	fuel flow, lb/hr
$W_g$	gas flow through combustion chamber, lb/sec
$W_y$	compressor-leakage air flow, lb/sec
$W_z$	turbine-cooling air flow, lb/sec
$\gamma$	ratio of specific heat at constant pressure to specific heat at constant volume
$\eta$	engine cycle efficiency
$\Delta\eta$	loss in engine cycle efficiency resulting from combustion-chamber pressure losses
$\eta_b$	combustion efficiency
$\theta_1$	ratio of engine-inlet total temperature to NACA standard sea-level static temperature
$\rho_T$	air density measured under total (stagnation) conditions, lb/cu ft

## Subscripts:

0	free stream
1	engine inlet
3	combustion-chamber inlet or compressor outlet
4	combustion-chamber outlet or turbine inlet
6	turbine outlet
7	exhaust-nozzle outlet
a	air
b	combustion chamber
f	fuel
j	station at which static pressure in jet reaches free-stream static pressure

## Methods of Calculation

Temperatures. - Static temperatures were obtained from indicated temperature readings by

$$t = \frac{T_1}{1 + 0.85 \left[ \left( \frac{P}{P_1} \right)^{\frac{\gamma-1}{\gamma}} - 1 \right]} \quad (1)$$

where 0.85 is the thermocouple impact recovery factor. Total temperatures were calculated from the adiabatic relation between pressures and static temperatures.

The equivalent free-stream static temperature  $t_0$  was calculated from the engine-inlet temperature and ram-pressure ratio as follows:

$$t_0 = T_1 \left( \frac{P_0}{P_1} \right)^{\frac{\gamma_1-1}{\gamma_1}} \quad (2)$$

The static temperature of the exhaust-gas jet was calculated from the tail-rake instrumentation by

$$t_j = t_7 \left( \frac{P_0}{P_7} \right)^{\frac{\gamma_7-1}{\gamma_7}} \quad (3)$$

No thermocouples were installed at the combustion-chamber outlet (station 4); in determining  $T_4$ , therefore, the enthalpy drop across the turbine was assumed equal to the measured enthalpy rise through the compressor corrected for variations of mass flow. The enthalpy at the turbine inlet is expressed as

$$H_4 = H_6 + \frac{W_{a,1}}{W_g} H_3 - H_1$$

The turbine-inlet temperature  $T_4$  was then obtained from a temperature-enthalpy chart.

Air flow. - Air flow was calculated from temperature and pressure measurements made at the engine inlet (station 1).

$$W_{a,1} = \frac{P_1 A_1}{R} \sqrt{\frac{2gJc_p}{t_1} \left[ \left( \frac{P_1}{P_1} \right)^{\frac{\gamma-1}{\gamma}} - 1 \right]} \quad (4)$$

where the value of  $A_1$  is 3.041 square feet.

Compressor-leakage air flow  $W_y$  and turbine-cooling air flow  $W_z$  were bled from the compressor; the resulting air flow entering the combustion chamber is therefore

$$W_{a,b} = W_{a,1} - W_y - W_z$$

and the gas flow leaving the combustion chamber is expressed as

$$W_g = W_{a,b} + \frac{W_f}{3600}$$

Combustion efficiency. - The combustion efficiency is defined as the ratio of the actual increase in the enthalpy of the gas while passing through the combustion chamber to the theoretical increase in enthalpy that would result from complete combustion of the fuel charge. Combustion efficiency was obtained from the expression

$$\eta_b = \frac{H_4(1 + f/a) - H_{a,3}}{(f/a) \times 18,550} \quad (5)$$

where the lower heating value of the fuel was 18,550 Btu per pound. The enthalpy values in this equation were obtained from  $T_3$  and  $T_4$  and a temperature-enthalpy chart based on a fuel-inlet temperature of 80° F and a hydrogen-carbon ratio of the fuel of 0.155 according to the method explained in reference 6.

Pressure losses. - The measured over-all total-pressure-loss ratio was determined from total-pressure measurements at the combustion-chamber inlet and the combustion-chamber outlet according to the expression

$$\frac{\Delta P_T}{P_3} = \frac{P_3 - P_4}{P_3} \quad (6)$$

The frictional and momentum pressure-loss ratios were determined by the method described in reference 5. This method involves the determination of the combustion-chamber friction pressure-loss factor  $K$  and the combustion-chamber equivalent area  $A_b$ . The friction pressure-loss factor  $K$  was determined from engine windmilling tests. The total-pressure losses obtained resulted from friction alone, inasmuch as no momentum pressure loss was introduced by heat addition. The friction pressure-loss factor  $K$  is defined by the relation

$$\Delta P_F = \frac{KW_{a,b}^2}{\rho_{T,3}} \quad (7a)$$

Therefore, using the perfect gas law,

$$K = \left( \frac{\Delta P_F}{P_3} \right) \left( \frac{P_3^2}{RW_{a,b}^2 T_3} \right) \quad (7b)$$

By use of this equation, the value of  $K$  was determined from windmilling data to be 0.007. The friction pressure-loss ratios were then calculated for the performance data using this value of  $K$  in the following equation

$$\frac{\Delta P_F}{P_3} = \frac{KW_{a,b}^2 T_3}{P_3^2} \quad (7c)$$

A tentative momentum pressure-loss ratio was then obtained by subtracting  $\Delta P_F/P_3$  from the measured total-pressure-loss ratio. By use of the pressure-loss chart, the values of  $\Delta P_F/P_3$ , the temperature ratio  $T_4/T_3$ , and the tentative momentum pressure-loss ratio, an average value of  $A_b$  of 0.273 square foot was established from performance data for several flight conditions. This constant value of  $A_b$  and the pressure-loss chart were then used to determine the momentum pressure-loss ratio  $\Delta P_M/P_3$  for all performance data. The calculated over-all total-pressure-loss ratio was determined by the relation

$$\frac{\Delta P_T}{P_3} = \frac{\Delta P_F}{P_3} + \frac{\Delta P_M}{P_3} \quad (8)$$



Engine cycle efficiency. - The engine cycle efficiency is defined by

$$\eta = \frac{\text{heat supplied to engine} - \text{heat rejected by engine}}{\text{heat supplied to engine}}$$

$$\eta = \frac{[H_4(1+f/a) - H_{a,3}] - c_p(t_j - t_0)}{[H_4(1+f/a) - H_{a,3}]} \quad (9)$$

where  $c_p$  is the average value between stations  $j$  and  $0$ .

The loss in engine cycle efficiency resulting from combustion-chamber pressure losses was calculated by the expression developed in reference 4:

$$\Delta\eta = \frac{c_p t_j \left[ 1 - \left( \frac{P_4}{P_3} \right)^{\frac{\gamma-1}{\gamma}} \right]}{[H_4(1+f/a) - H_{a,3}]} \quad (10)$$

where  $c_p$  is the average value between stations  $j$  and  $0$  and  $\gamma$  is the average value between stations  $4$  and  $j$ .

#### REFERENCES

1. Conrad, E. William, and Sobolewski, Adam E.: Altitude-Wind-Tunnel Investigation of J47 Turbojet-Engine Performance. NACA RM E9G09, 1949.
2. Prince, William R., and Jansen, Emmert T.: Altitude-Wind-Tunnel Investigation of Compressor Performance on J47 Turbojet Engine. NACA RM E9G28, 1949.
3. Thorman, H. Carl, and McAulay, John E.: Altitude-Wind-Tunnel Investigation of Turbine Performance in J47 Turbojet Engine. NACA RM E9K10, 1950.
4. Pinkel, I. Irving, and Shames, Harold: Altitude-Wind-Tunnel Investigation of a 4000-Pound-Thrust Axial-Flow Turbojet Engine. VI - Combustion-Chamber Performance. NACA RM E8F09e, 1948.

5. Pinkel, I. Irving, and Shames, Harold: Analysis of Jet-Propulsion-Engine Combustion-Chamber Pressure Losses. NACA Rep. 880, 1947. (Formerly NACA TN 1180.)
6. Turner, L. Richard, and Lord, Albert M.: Thermodynamic Charts for the Computation of Combustion and Mixture Temperatures at Constant Pressure. NACA TN 1086, 1946.

TABLE I - COMBUSTION-CHAMBER PERFORMANCE

Run	Altitude (ft.)	Ram pressure ratio, $P_1/P_0$	Flight Mach number	Tunnel static pressure, $P_0$ (lb/sq ft abs.)	Engine speed, N (rpm)	Corrected engine speed, $N/\sqrt{\sigma_1}$ (rpm) <sup>a</sup>	Compressor-inlet total temperature, $T_1$ , (°R)	Combustion-chamber-inlet total pressure, $P_3$ (lb/sq ft abs.)	Combustion-chamber-inlet total temperature, $T_3$ (°R)	Combustion-chamber- outlet total pressure, $P_4$ (lb/sq ft abs.)	Combustion-chamber- outlet total temperature, $T_4$ (°R)	Turbine-outlet total pressure, $P_5$ (lb/sq ft abs.)	Turbine-outlet total temperature, $T_5$ (°R)	Exhaust-nozzle-outlet static pressure, $P_7$ (lb/sq ft abs.)
Exhaust-nozzle outlet area, 280 square inches														
1	5,000	1.038	0.230	1740	7895	7950	512	9339	900	8977	2080	3465	1740	2198
2	5,000	1.037	.228	1756	7692	7730	514	9095	884	8726	1960	3352	1631	2147
3	5,000	1.039	.230	1740	7500	7553	512	8759	873	8599	1869	3247	1542	2076
4	5,000	1.036	.220	1742	6993	7035	513	7980	838	7857	1694	2984	1396	1965
5	5,000	1.033	.210	1744	5944	5992	511	5874	754	5627	1397	2403	1170	1820
6	5,000	1.033	.210	1740	5024	5069	510	4215	663	4045	1263	2083	1096	1771
7	5,000	1.034	.215	1749	4091	4132	509	3066	621	2954	1238	1924	1125	1766
8	5,000	1.032	.210	1745	3147	3178	509	2412	574	2353	1230	1832	1167	1750
9	5,000	1.032	.210	1738	2046	2068	509	1993	532	1966	1161	1769	1134	1740
10	15,000	1.204	.525	1186	7895	8045	500	7262	900	7002	2100	2665	1754	1680
11	15,000	1.210	.530	1186	7692	7808	504	7190	878	6898	1945	2625	1614	1646
12	15,000	1.211	.530	1186	7500	7590	507	6966	865	6681	1865	2549	1544	1593
13	15,000	1.205	.525	1190	6993	7084	506	6359	829	6101	1658	2334	1362	1470
14	15,000	1.203	.520	1188	6459	6530	508	5459	789	5257	1459	2029	1200	1352
15	15,000	1.203	.520	1190	5944	6021	506	4570	744	4369	1287	1765	1058	1261
16	15,000	1.204	.525	1188	5024	5094	508	3168	665	3028	1065	1458	914	1209
17	15,000	1.203	.520	1190	4091	4140	507	2259	603	2162	975	1340	890	1209
18	15,000	1.203	.520	1190	3147	3194	504	1706	552	1642	860	1258	801	1202
19	25,000	1.037	.225	777	7692	8238	452	4451	845	4300	2120	1661	1783	1047
20	25,000	1.037	.225	774	7500	8010	455	4188	818	4028	1899	1549	1680	985
21	25,000	1.036	.220	777	6993	7462	456	3873	778	3713	1690	1435	1588	986
22	25,000	1.033	.210	778	6459	6898	455	3485	741	3345	1500	1310	1244	873
23	25,000	1.033	.210	778	5944	6342	456	2976	708	2856	1350	1185	1121	829
24	25,000	1.031	.205	778	5024	5366	455	2103	632	2021	1190	972	1011	801
25	25,000	1.030	.205	777	4091	4565	456	1498	574	1442	1150	870	1034	788
26	25,000	1.030	.205	774	3147	3358	456	1127	521	1098	1155	815	1095	779
27	25,000	1.030	.205	774	2046	2185	455	909	485	895	1185	790	1152	774
28	25,000	1.207	.526	781	7895	8313	468	6137	878	4955	2156	1900	1781	1191
29	25,000	1.209	.530	774	7692	8115	466	4985	850	4795	2000	1834	1661	1146
30	25,000	1.211	.530	781	7500	8003	466	4912	818	4717	1967	1811	1640	1129
31	25,000	1.213	.535	774	6993	7462	456	4525	773	4540	1642	1658	1559	1037
32	25,000	1.211	.530	778	6459	6872	458	4006	736	3848	1450	1469	1200	941
33	25,000	1.208	.530	785	5944	6315	460	3408	697	3263	1266	1269	1045	860
34	25,000	1.203	.520	778	5024	5300	466	2356	627	2251	1090	999	900	804
35	25,000	1.202	.520	781	4091	4516	466	1675	566	1506	936	885	831	792
36	25,000	1.199	.515	778	2727	2888	463	1060	498	1024	790	816	753	784
37	25,000	1.412	.720	774	7895	8308	469	5921	868	5717	2106	2199	1783	1347
38	25,000	1.403	.715	776	7692	8038	475	5759	855	5546	2008	2133	1673	1329
39	25,000	1.403	.715	781	7500	7815	478	5529	834	5308	1845	2022	1630	1262
40	25,000	1.413	.720	780	6993	7287	478	5115	798	4909	1649	1867	1558	1160
41	25,000	1.410	.720	783	6459	6737	477	4486	757	4295	1432	1631	1174	1014
42	25,000	1.415	.725	781	5944	6182	480	3657	715	3498	1208	1350	982	884
43	25,000	1.406	.720	781	5024	5240	477	2499	634	2366	935	1036	780	810
44	25,000	1.611	.855	774	7800	7658	498	6123	858	5872	1863	2237	1546	1395
45	25,000	1.611	.855	781	6993	7119	501	5621	822	5395	1651	2048	1359	1269
46	25,000	1.609	.850	781	6459	6575	501	4829	779	4625	1417	1744	1157	1087
47	25,000	1.603	.850	781	5944	6069	498	3899	726	3724	1155	1416	941	909
48	25,000	1.612	.855	781	5024	5109	502	2599	653	2463	875	1059	717	813
49	25,000	1.857	.982	746	7895	8029	502	7185	886	6909	2038	2659	1705	1584
50	25,000	1.817	.965	778	7692	7754	511	7088	881	6903	1955	2596	1629	1556
51	25,000	1.839	.978	774	7500	7545	513	6902	873	6680	1870	2532	1554	1556
52	25,000	1.840	.975	774	6993	7028	514	6250	837	5974	1655	2292	1365	1400
53	35,000	1.032	.210	498	7692	8315	444	2882	844	2766	2150	1063	1814	671
54	35,000	1.034	.215	493	7500	8100	445	2717	824	2616	2015	1010	1681	658
55	35,000	1.036	.220	498	6993	7545	446	2515	776	2414	1725	928	1428	596
56	35,000	1.032	.210	496	6459	6978	445	2256	737	2170	1535	846	1273	559
57	35,000	1.030	.205	495	5944	6490	445	1903	696	1827	1370	740	1138	530
58	35,000	1.030	.205	494	5024	5426	445	1385	626	1329	1190	617	1018	508
59	35,000	1.028	.195	497	4091	4414	446	980	568	944	1185	563	1062	509
60	35,000	1.204	.525	494	7692	8277	448	3239	840	3124	2060	1199	1723	751
61	35,000	1.211	.530	493	7500	8070	448	3142	817	3023	1916	1189	1598	725
62	35,000	1.208	.530	495	6993	7517	449	2876	773	2754	1676	1056	1586	661

<sup>a</sup>Engine speed corrected to NACA standard sea-level static conditions.<sup>b</sup>Calculated values obtained by using pressure-loss chart developed in reference 5.<sup>c</sup>Data omitted.

1218

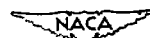
NACA

DATA FOR J47 TURBOJET ENGINE

Exhaust-nozzle-outlet static temperature, $T_9$ (°R)	Fuel flow, $W_f$ (lb/hr)	Engine-inlet air flow, $W_{a,i}$ (lb/sec)	Combustion-chamber air flow, $W_{a,b}$ (lb/sec)	Combustion-chamber fuel-air ratio, $f/a$	Combustion efficiency, $\eta_b$	Measured over-all total-pressure-loss ratio, $\Delta P_T/P_3$	Calculated over-all total-pressure-loss ratio, $\Delta P_T/P_3$	Friction pressure-loss ratio, $\Delta P_f/P_3$	Momentum pressure-loss ratio, $\Delta P_m/P_3$	Engine-cycle efficiency, $\eta$	Fractional loss in engine-cycle efficiency, $\Delta\eta/\eta$	Run
Exhaust-nozzle outlet area, 280 square inches												
1568	5300	81.08	78.92	0.0187	0.952	0.0388	0.0394	0.0240	0.0154	0.245	0.045	1
1470	4800	81.07	79.00	0.0169	0.951	0.0406	0.0398	0.0249	0.0149	0.241	0.051	2
1388	4390	80.28	78.17	0.0156	0.947	0.0411	0.0408	0.0260	0.0148	0.242	0.053	3
1284	3550	76.94	75.03	0.0131	0.951	0.0405	0.0413	0.0276	0.0137	0.221	0.063	4
1091	2060	63.66	62.44	0.0092	0.979	0.0421	0.0455	0.0319	0.0136	0.151	0.116	5
1052	1350	48.05	47.03	0.0080	0.991	0.0408	0.0454	0.0318	0.0136	0.089	0.218	6
1101	1050	34.21	33.23	0.0088	0.963	0.0365	0.0403	0.0273	0.0130	0.082	0.272	7
1153	820	23.73	22.79	0.0100	0.995	0.0231	0.0293	0.0190	0.0103	0.028	0.374	8
1129	474	16.42	15.49	0.0086	(c)	0.0135	0.0186	0.0120	0.0068	0.008	(c)	9
1577	4130	62.37	60.59	0.0169	0.958	0.0358	0.0385	0.0234	0.0151	0.260	0.037	10
1446	3730	64.50	62.75	0.0165	0.961	0.0408	0.0398	0.0249	0.0149	0.265	0.044	11
1383	3395	64.09	62.59	0.0151	0.975	0.0409	0.0404	0.0259	0.0145	0.259	0.048	12
1318	2720	61.72	60.17	0.0126	0.960	0.0406	0.0412	0.0277	0.0138	0.244	0.056	13
1081	1990	56.77	55.48	0.0100	0.938	0.0424	0.0450	0.0303	0.0127	0.193	0.087	14
971	1380	50.82	49.75	0.0077	0.973	0.0440	0.0449	0.0329	0.0120	0.158	0.128	15
870	770	38.87	38.18	0.0056	0.972	0.0442	0.0470	0.0360	0.0110	0.067	0.382	16
867	649	27.95	27.54	0.0056	0.876	0.0429	0.0453	0.0330	0.0103	0.002	(c)	17
792	561	21.99	21.75	0.0046	0.867	0.0375	0.0428	0.0334	0.0091	(c)	(c)	18
1607	2610	38.58	37.47	0.0184	0.955	0.0339	0.0384	0.0223	0.0161	0.262	0.035	19
1421	2200	38.02	37.27	0.0164	0.973	0.0382	0.0399	0.0248	0.0157	0.245	0.045	20
1249	1780	37.39	36.62	0.0135	0.966	0.0413	0.0408	0.0260	0.0148	0.235	0.056	21
1126	1420	35.59	34.90	0.0113	0.950	0.0402	0.0415	0.0278	0.0137	0.200	0.073	22
1031	1070	31.96	31.27	0.0095	0.942	0.0403	0.0420	0.0290	0.0130	0.166	0.099	23
961	702	24.64	24.12	0.0081	0.938	0.0390	0.0446	0.0311	0.0135	0.126	0.141	24
1008	580	18.10	17.58	0.0089	0.872	0.0374	0.0439	0.0295	0.0144	0.055	0.320	25
1082	440	12.24	11.75	0.0104	0.824	0.0287	0.0335	0.0211	0.0124	0.020	0.581	26
1146	368	8.70	8.22	0.0124	0.770	0.0154	0.0250	0.0148	0.0102	0.023	0.293	27
1602	3025	44.86	43.07	0.0195	0.976	0.0354	0.0390	0.0231	0.0159	0.277	0.033	28
1490	2725	44.25	43.20	0.0175	0.980	0.0385	0.0395	0.0238	0.0157	0.276	0.038	29
1386	2550	45.17	44.19	0.0160	0.967	0.0397	0.0403	0.0246	0.0157	0.273	0.041	30
1213	2030	44.24	43.49	0.0130	0.958	0.0409	0.0412	0.0267	0.0145	0.253	0.051	31
1075	1590	41.79	41.09	0.0107	0.937	0.0394	0.0427	0.0290	0.0137	0.218	0.065	32
946	1139	38.14	37.54	0.0084	0.937	0.0417	0.0445	0.0316	0.0129	0.182	0.097	33
850	600	28.06	27.51	0.0061	0.955	0.0445	0.0459	0.0325	0.0114	0.098	0.240	34
807	425	21.02	20.48	0.0058	0.846	0.0438	0.0478	0.0357	0.0118	0.031	0.861	35
745	266	13.71	13.16	0.0056	0.684	0.0340	0.0372	0.0287	0.0085	(c)	(c)	36
1577	3410	51.82	50.34	0.0188	0.992	0.0345	0.0395	0.0234	0.0161	0.304	0.028	37
1801	3150	50.79	49.40	0.0177	0.972	0.0370	0.0388	0.0235	0.0153	0.302	0.032	38
1368	2750	50.75	49.44	0.0154	0.963	0.0400	0.0398	0.0249	0.0149	0.291	0.039	39
1211	2220	50.34	49.15	0.0125	0.979	0.0403	0.0419	0.0275	0.0144	0.279	0.045	40
1044	1660	47.59	46.59	0.0098	0.953	0.0426	0.0440	0.0306	0.0138	0.235	0.067	41
881	1020	43.26	42.45	0.0067	(c)	0.0435	0.0488	0.0360	0.0128	0.186	0.107	42
731	469	32.96	32.44	0.0040	(c)	0.0494	0.0500	0.0403	0.0097	0.059	0.559	43
1383	3050	56.50	54.98	0.0154	0.959	0.0410	0.0410	0.0259	0.0151	0.289	0.037	44
1211	2420	54.06	52.88	0.0128	0.955	0.0402	0.0401	0.0270	0.0151	0.294	0.045	45
1027	1680	50.99	49.88	0.0094	0.946	0.0422	0.0437	0.0310	0.0127	0.248	0.064	46
838	970	45.33	44.45	0.0061	0.984	0.0449	0.0458	0.0353	0.0105	0.168	0.135	47
669	346	35.63	35.04	0.0027	(c)	0.0504	0.0523	0.0444	0.0079	(c)	(c)	48
1512	4000	63.45	61.80	0.0180	0.962	0.0357	0.0402	0.0245	0.0157	0.346	0.026	49
1454	3730	63.95	62.16	0.0167	0.962	0.0402	0.0408	0.0253	0.0153	0.340	0.031	50
1386	3400	63.83	62.17	0.0152	0.968	0.0409	0.0415	0.0265	0.0150	0.331	0.034	51
1213	2640	61.07	59.52	0.0123	0.960	0.0411	0.0419	0.0288	0.0134	0.311	0.041	52
1636	1719	24.42	23.88	0.0200	0.999	0.0335	0.0381	0.0219	0.0162	0.247	0.035	53
1513	1505	24.43	23.85	0.0175	1.013	0.0372	0.0404	0.0237	0.0167	0.245	0.041	54
1286	1184	24.05	23.48	0.0140	0.982	0.0402	0.0406	0.0253	0.0153	0.239	0.054	55
1161	944	22.87	22.30	0.0118	0.960	0.0381	0.0409	0.0269	0.0140	0.202	0.066	56
1747	723	20.57	20.13	0.0100	0.958	0.0399	0.0428	0.0291	0.0137	0.188	0.093	57
970	497	15.99	15.57	0.0089	0.866	0.0397	0.0428	0.0296	0.0132	0.104	0.172	58
1036	381	11.23	10.87	0.0097	0.882	0.0367	0.0401	0.0261	0.0140	0.066	0.246	59
1548	1870	28.55	27.89	0.0186	0.982	0.0355	0.0397	0.0233	0.0164	0.273	0.034	60
1451	1690	28.66	28.00	0.0168	0.966	0.0379	0.0399	0.0242	0.0157	0.268	0.039	61
1240	1300	28.26	27.64	0.0131	0.988	0.0424	0.0418	0.0267	0.0151	0.247	0.053	62

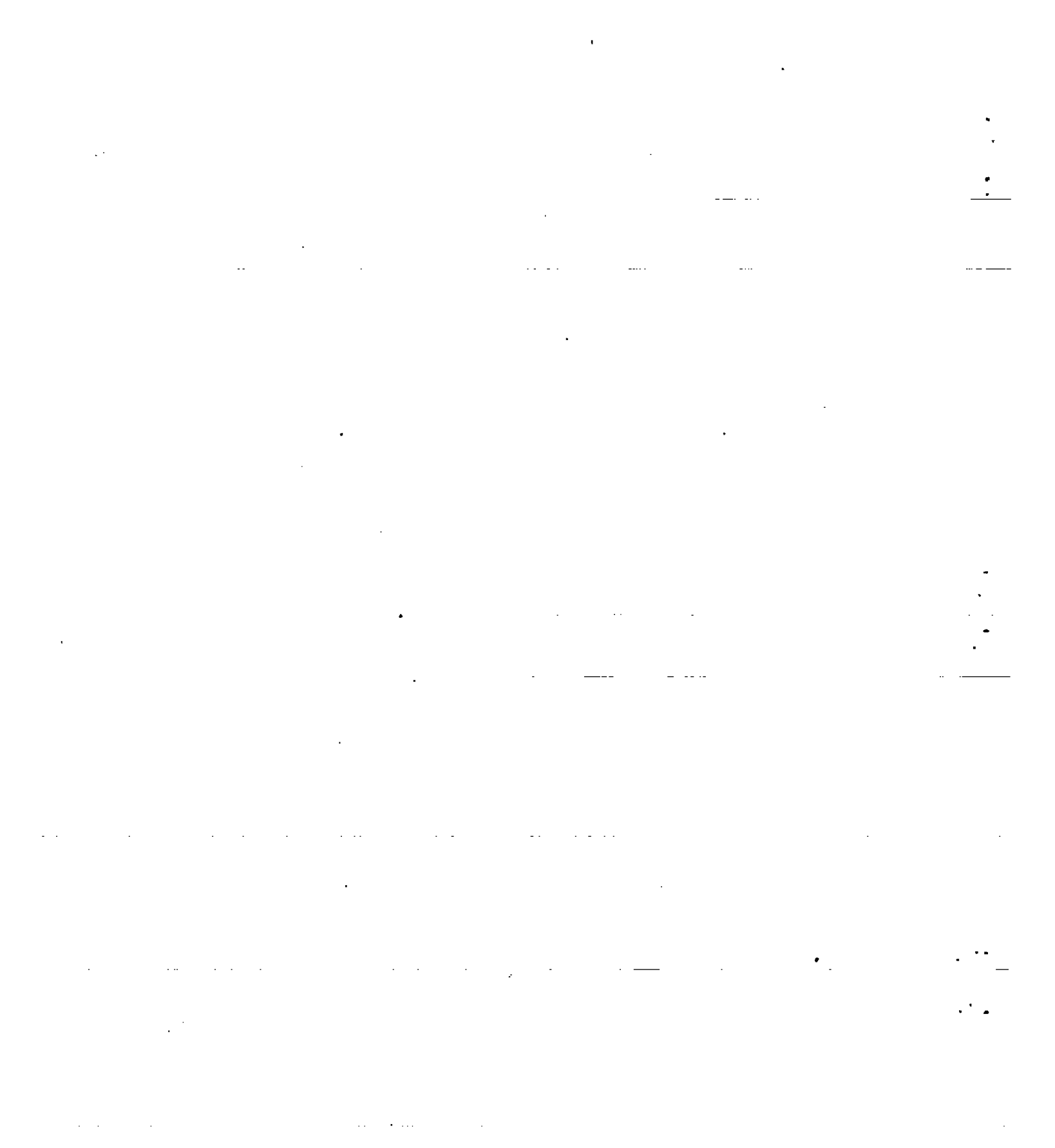
TABLE I - COMBUSTION-CHAMBER PERFORMANCE

Run	Altitude (ft)	Ram pressure ratio, $P_2/P_0$	Flight Mach number	Tunnel static pressure, $P_0$ (lb/sq ft abs.)	Engine speed, $N$ (rpm)	Corrected engine speed, $N/\sqrt{P_2}$ , (rpm) <sup>a</sup>	Compressor-inlet total temperature, $T_2$ , (°R)	Combustion-chamber-inlet total pressure, $P_3$ (lb/sq ft abs.)	Combustion-chamber-inlet total temperature, $T_3$ (°R)	Combustion-chamber- outlet total pressure, $P_4$ (lb/sq ft abs.)	Combustion-chamber- outlet total tempera- ture, $T_4$ , (°R)	Turbine-outlet total pressure, $P_5$ (lb/sq ft abs.)	Turbine-outlet total temperature, $T_5$ , (°R)	Exhaust-nozzle-outlet static pressure, $P_y$ (lb/sq ft abs.)
Exhaust-nozzle outlet area, 280 square inches - Concluded														
63	35,000	1.200	0.520	496	6459	6956	447	3566	733	2463	1470	945	1213	600
64	35,000	1.202	.520	496	5944	6596	448	2182	691	2091	1276	817	1051	550
65	35,000	1.198	.516	495	5024	5421	446	1506	614	1458	1037	644	878	515
66	35,000	1.409	.720	494	7800	8593	448	5843	852	3705	2124	1427	1782	892
67	35,000	1.411	.720	494	7692	8284	447	5784	838	3582	2081	1403	1724	874
68	35,000	1.411	.720	496	7500	8093	446	5626	811	3522	1902	1350	1579	839
69	35,000	1.413	.720	496	6993	7652	445	5410	765	3270	1655	1236	1373	768
70	35,000	1.407	.720	496	6459	6982	444	5019	728	2900	1449	1101	1197	683
71	35,000	1.411	.720	494	5944	6443	442	2538	681	2430	1230	924	998	594
72	35,000	1.405	.715	496	5455	5913	442	2075	637	1982	1032	772	849	536
73	45,000	1.037	.225	298	7500	8130	442	1714	835	1657	2130	637	1793	404
74	45,000	1.029	.200	308	6993	7545	446	1561	786	1505	1810	582	1510	376
75	45,000	1.037	.225	297	6459	6995	443	1374	740	1322	1582	510	1318	344
76	45,000	1.033	.210	306	5944	6420	445	1181	701	1134	1416	466	1178	359
77	45,000	1.030	.205	303	5024	5431	444	852	632	802	1260	378	1078	316
78	45,000	1.206	.528	301	7692	8307	445	1992	851	1927	2179	750	1830	474
79	45,000	1.209	.530	301	7500	8093	446	1925	828	1858	2035	713	1710	451
80	45,000	1.198	.515	303	6993	7559	444	1752	776	1686	1745	648	1456	416
81	45,000	1.204	.525	304	6459	6995	443	1572	730	1611	1510	578	1253	370
82	45,000	1.205	.525	303	5944	6437	443	1327	690	1275	1315	502	1087	344
83	45,000	1.203	.520	296	5024	5441	443	909	619	872	1080	388	915	311
84	50,000	1.027	.190	225	7500	8123	443	1276	842	1259	2145	469	1812	300
85	50,000	1.025	.185	236	6993	7573	443	1204	799	1159	1888	446	1554	290
86	50,000	1.025	.185	238	6459	7008	441	1067	739	1031	1610	404	1346	271
87	50,000	1.025	.185	239	5944	6455	440	936	701	901	1458	365	1221	260
Exhaust-nozzle outlet area, 302 square inches														
88	5,000	1.036	0.220	1740	7895	8077	496	6928	868	5573	1817	3066	1485	1978
89	5,000	1.033	.215	1745	7692	7881	497	6637	852	5301	1733	2993	1415	1946
90	5,000	1.038	.220	1753	7500	7658	498	6440	840	5105	1652	2936	1351	1927
91	5,000	1.033	.215	1747	6993	7133	499	7770	807	7456	1516	2742	1236	1859
92	5,000	1.030	.206	1745	6459	6876	501	6865	789	6581	1389	2495	1138	1810
93	5,000	1.030	.206	1745	5944	6051	501	5867	733	5612	1290	2306	1071	1784
94	5,000	1.030	.206	1754	5024	5114	501	4278	667	4096	1170	2087	1013	1776
95	5,000	1.029	.198	1748	4091	4173	499	3093	611	2975	1155	1906	1052	1763
96	5,000	1.028	.196	1745	3147	3213	498	2427	562	2355	1162	1827	1101	1752
97	5,000	1.029	.198	1748	2046	2091	497	2012	525	1982	1119	1779	1097	1753
98	25,000	1.031	.203	788	7895	8400	458	4231	847	4079	1900	1467	1555	923
99	25,000	1.032	.203	781	7692	8169	460	4032	824	3872	1783	1397	1440	903
100	25,000	1.031	.203	781	7500	7980	458	3926	805	3770	1668	1357	1356	885
101	25,000	1.029	.200	781	6993	7441	458	3551	766	3502	1497	1278	1220	851
102	25,000	1.029	.200	781	6459	6918	452	3329	726	3196	1361	1192	1107	826
103	25,000	1.029	.200	781	5024	5391	451	2085	620	1999	1092	943	935	796
104	25,000	1.028	.198	781	4091	4349	459	1466	569	1411	1102	866	993	793
105	25,000	1.032	.203	783	3147	3336	462	1114	523	1080	1110	823	1050	704
106	25,000	1.031	.203	774	2046	2167	465	903	493	891	1086	788	1066	777
Exhaust-nozzle outlet area, 342 square inches														
107	5,000	1.034	0.215	1752	7895	8084	495	6448	854	5137	1832	2686	1308	1801
108	5,000	1.032	.210	1745	7692	7889	498	6237	838	7897	1584	2648	1252	1794
109	5,000	1.030	.210	1753	6993	7140	498	7481	794	7186	1372	2493	1100	1784
110	5,000	1.027	.195	1753	6459	6601	497	6655	763	6364	1282	2307	1036	1779
111	5,000	1.030	.210	1741	5944	6078	497	6738	728	5486	1206	2147	988	1761
112	5,000	1.029	.200	1733	5024	5138	497	4227	683	4042	1115	1932	957	1760
113	5,000	1.029	.200	1744	4091	4177	498	3060	605	2957	1108	1860	1006	1746
114	5,000	1.029	.200	1744	3147	3219	496	2397	560	2327	1120	1806	1060	1744
115	5,000	1.029	.200	1742	2046	2095	495	1982	519	1954	1075	1765	1048	1742
116	25,000	1.032	.210	781	7895	8361	463	3938	834	3781	1636	1212	1311	804
117	25,000	1.032	.210	781	7692	8148	463	3827	819	3668	1587	1190	1265	804
118	25,000	1.031	.210	778	7500	7943	463	3697	800	3545	1493	1189	1206	801
119	25,000	1.029	.200	781	6993	7413	462	3490	765	3348	1382	1112	1100	801
120	25,000	1.028	.200	781	6459	6853	461	3163	730	3028	1271	1060	1010	799
121	25,000	1.027	.195	780	5944	6313	460	2789	696	2636	1175	996	946	791
122	25,000	1.027	.195	780	5024	5341	459	2012	627	1926	1064	889	902	789
123	25,000	1.028	.200	781	4091	4349	459	1433	565	1379	1058	837	947	784
124	25,000	1.028	.200	776	3147	3348	459	1134	524	1082	1081	802	1019	779

<sup>a</sup>Engine speed corrected to NACA standard sea-level static conditions.<sup>b</sup>Calculated values obtained by using pressure-loss chart developed in reference 5.<sup>c</sup>Data omitted.

## DATA FOR J47 TURBOJET ENGINE - Concluded

Exhaust-nozzle-outlet static temperature, $t_e$ (°R)	Fuel flow, $W_f$ (lb/hr)	Engine-inlet air flow, $W_a$ (lb/sec)	Combustion-chamber air flow, $W_{a,b}$ (lb/sec)	Combustion-chamber fuel-air ratio, $f/a$	Combustion efficiency, $\eta_b$	Measured over-all total-pressure-loss ratio, $\Delta P_T/P_3$	Calculated over-all total-pressure-loss ratio, $\Delta P_T/P_3$	Friction pressure-loss ratio, $\Delta P_F/P_3$	Momentum pressure-loss ratio, $\Delta P_M/P_3$	Engine-cycle efficiency, $\eta$	Fractional loss in engine-cycle efficiency, $\Delta\eta/\eta$	Run
Exhaust-nozzle outlet area, 280 square inches - Concluded												
1085	1000	26.25	25.63	0.0108	0.959	0.0402	0.0405	0.0274	0.0131	0.218	0.066	63
951	760	24.32	23.93	.0088	.919	.0417	.0441	.0311	.0130	.181	.098	64
828	430	15.82	15.50	.0065	.879	.0445	.0468	.0347	.0121	.098	.255	65
1601	2295	33.74	32.88	.0194	.992	.0359	.0401	.0233	.0168	.305	.029	66
1547	2165	33.83	32.96	.0182	1.007	.0349	.0406	.0237	.0169	.308	.029	67
1413	1950	34.14	33.38	.0162	.992	.0287	.0424	.0257	.0167	.298	.025	68
1224	1550	33.76	33.02	.0130	.987	.0411	.0419	.0268	.0151	.279	.044	69
1064	1175	32.19	31.50	.0104	.975	.0394	.0438	.0295	.0145	.246	.055	70
891	820	29.09	28.61	.0080	.937	.0426	.0454	.0324	.0150	.214	.082	71
771	544	26.10	25.69	.0059	.914	.0448	.0481	.0365	.0116	.142	.182	72
1618	1030	14.72	14.28	.0201	.978	.0333	.0374	.0216	.0158	.252	.034	73
1364	788	14.43	13.96	.0157	.955	.0359	.0384	.0235	.0149	.226	.047	74
1198	615	13.78	13.33	.0128	.939	.0378	.0405	.0260	.0145	.201	.063	75
1088	474	12.42	11.97	.0110	.907	.0398	.0402	.0269	.0133	.173	.087	76
1031	326	9.81	9.37	.0097	.884	.0361	.0444	.0299	.0145	.101	.155	77
1651	1225	17.28	16.80	.0203	.993	.0326	.0397	.0226	.0171	.279	.029	78
1540	1093	17.15	16.68	.0182	.989	.0348	.0395	.0232	.0163	.263	.035	79
1312	847	16.67	16.27	.0145	.970	.0377	.0403	.0250	.0153	.245	.046	80
1125	655	16.18	15.83	.0115	.956	.0388	.0421	.0276	.0145	.212	.065	81
989	497	14.87	14.62	.0094	.918	.0392	.0453	.0313	.0140	.176	.089	82
865	271	11.35	11.16	.0067	.933	.0407	.0482	.0349	.0133	.088	.230	83
1637	773	10.97	10.72	.0200	.986	.0290	.0388	.0222	.0164	.240	.031	84
1406	637	11.00	10.75	.0165	.951	.0374	.0388	.0235	.0153	.224	.049	85
1224	493	10.34	10.11	.0135	.922	.0337	.0392	.0248	.0144	.195	.068	86
1124	416	9.62	9.39	.0123	.864	.0374	.0401	.0263	.0138	.165	.083	87
Exhaust nozzle outlet area, 302 square inches												
1341	4320	81.86	79.77	0.0150	0.931	0.0398	0.0397	0.0259	0.0139	0.215	0.060	88
1280	3910	81.82	79.84	.0136	.940	.0359	.0408	.0272	.0136	.202	.065	89
1224	3600	81.63	79.92	.0125	.940	.0397	.0412	.0281	.0131	.195	.072	90
1127	3000	78.55	76.80	.0108	.934	.0404	.0422	.0294	.0129	.182	.086	91
1050	2400	72.30	70.76	.0094	.918	.0414	.0427	.0305	.0122	.160	.111	92
1006	1850	64.11	62.81	.0082	.940	.0434	.0432	.0315	.0119	.133	.153	93
977	1250	49.38	48.54	.0070	.978	.0425	.0441	.0321	.0120	.078	.288	94
1032	999	36.38	35.94	.0077	.959	.0351	.0444	.0308	.0136	.037	.518	95
1089	768	28.40	28.08	.0065	.862	.0297	.0339	.0224	.0115	.020	.720	96
1093	502	18.06	14.89	.0094	.849	.0149	.0169	.0107	.0052	(c)		97
1423	2200	37.77	36.80	.0166	.942	.0359	.0387	.0240	.0147	.209	.051	98
1317	1940	37.39	36.49	.0148	.929	.0397	.0393	.0252	.0141	.199	.063	99
1239	1760	37.31	36.47	.0134	.924	.0397	.0395	.0260	.0135	.196	.068	100
1119	1450	36.54	35.76	.0113	.916	.0408	.0399	.0274	.0125	.173	.088	101
1022	1190	35.28	34.59	.0096	.921	.0400	.0419	.0293	.0126	.159	.102	102
900	660	24.49	24.14	.0076	.844	.0415	.0429	.0311	.0118	.078	.269	103
973	513	18.93	18.71	.0085	.844	.0375	.0403	.0276	.0127	.049	.577	104
1042	425	12.32	12.17	.0097	.812	.0305	.0359	.0233	.0126	.018	.816	105
1062	341	7.67	7.59	.0125	.647	.0133	.0204	.0129	.0075	.003	(c)	106
Exhaust-nozzle outlet area, 343 square inches												
1199	3450	82.17	80.24	0.0119	0.942	0.0368	0.0418	0.0288	0.0130	0.160	0.086	107
1152	3200	81.30	79.46	.0112	.929	.0415	.0416	.0291	.0125	.159	.101	108
1023	2470	75.42	76.78	.0089	.903	.0421	.0427	.0313	.0114	.135	.141	109
974	1990	72.30	71.34	.0077	.931	.0434	.0442	.0328	.0114	.117	.181	110
942	1675	64.61	63.39	.0069	.961	.0439	.0442	.0331	.0111	.112	.201	111
930	1100	49.49	48.67	.0063	.967	.0438	.0442	.0328	.0114	.055	.443	112
991	910	36.37	35.84	.0071	.942	.0357	.0458	.0310	.0128	.014	(c)	113
1051	783	23.97	23.76	.0089	.842	.0292	.0303	.0206	.0097	.005	(c)	114
1045	450	15.05	14.99	.0083	.896	.0141	.0165	.0111	.0084	.008	(c)	115
1195	1681	37.53	36.65	.0127	.913	.0399	.0393	.0270	.0123	.156	.092	116
1156	1556	37.28	36.46	.0119	.929	.0416	.0406	.0278	.0125	.163	.093	117
1108	1417	37.01	36.44	.0108	.908	.0411	.0415	.0290	.0125	.130	.125	118
1016	1204	36.37	35.65	.0094	.912	.0407	.0417	.0298	.0119	.145	.118	119
943	988	34.82	34.19	.0080	.923	.0427	.0459	.0319	.0120	.139	.140	120
895	818	31.60	30.96	.0073	.901	.0444	.0443	.0328	.0115	.129	.170	121
877	590	23.99	23.64	.0068	.872	.0427	.0437	.0324	.0113	.071	.326	122
933	474	16.94	16.74	.0079	.838	.0377	.0411	.0288	.0123	.032	.610	123
1012	401	11.60	11.76	.0095	.789	.0635	.0318	.0211	.0107	.010	(c)	124



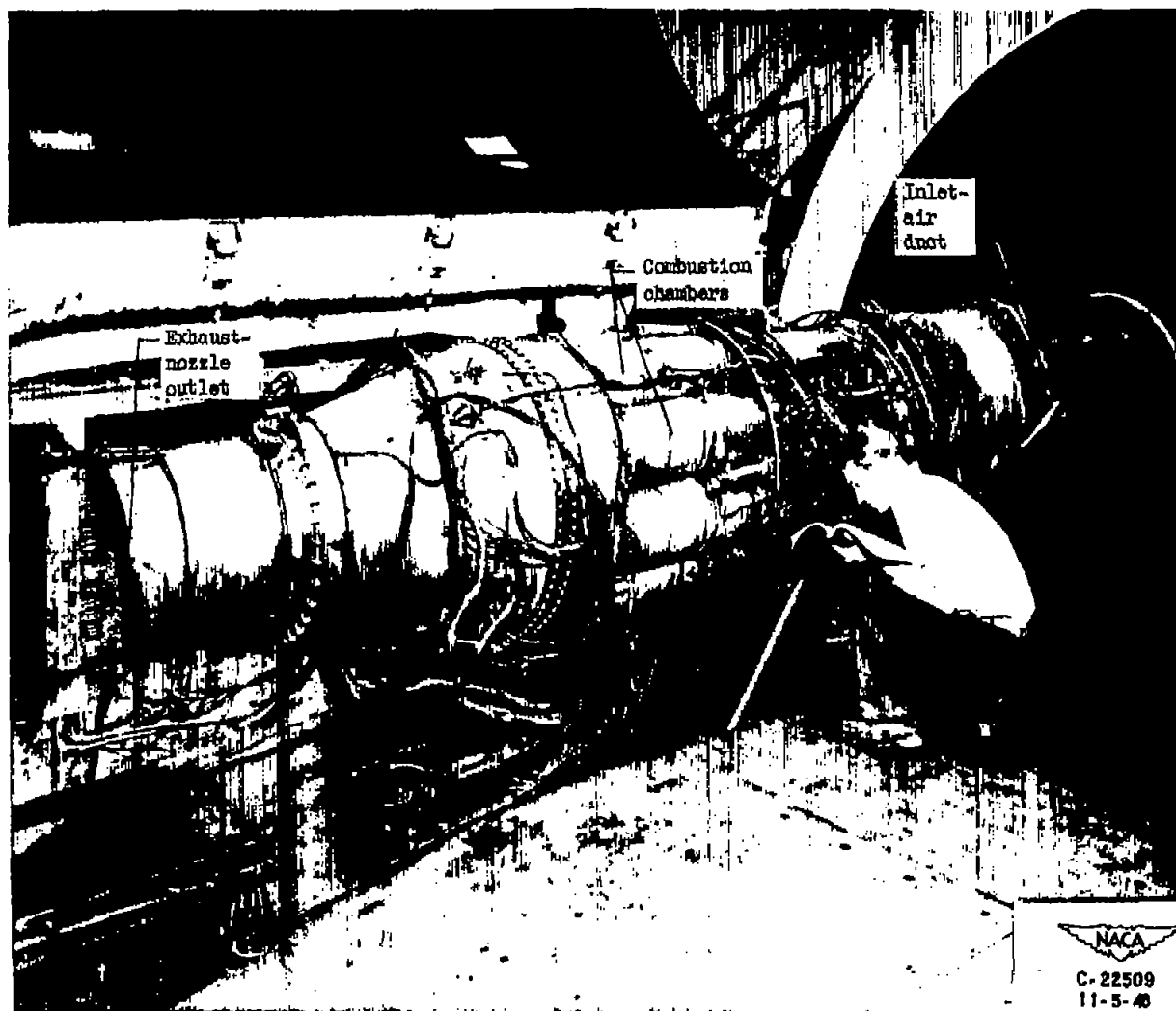
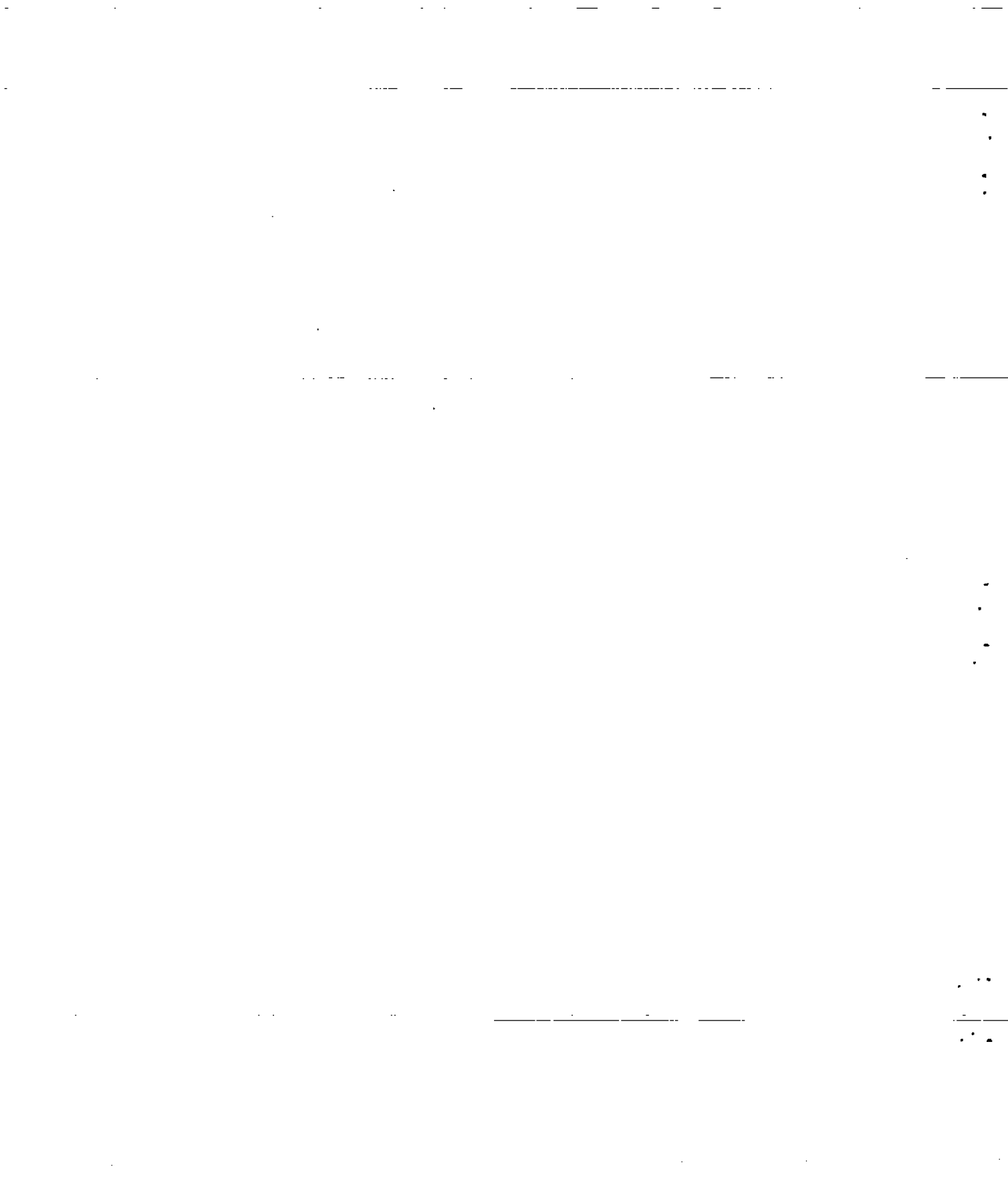
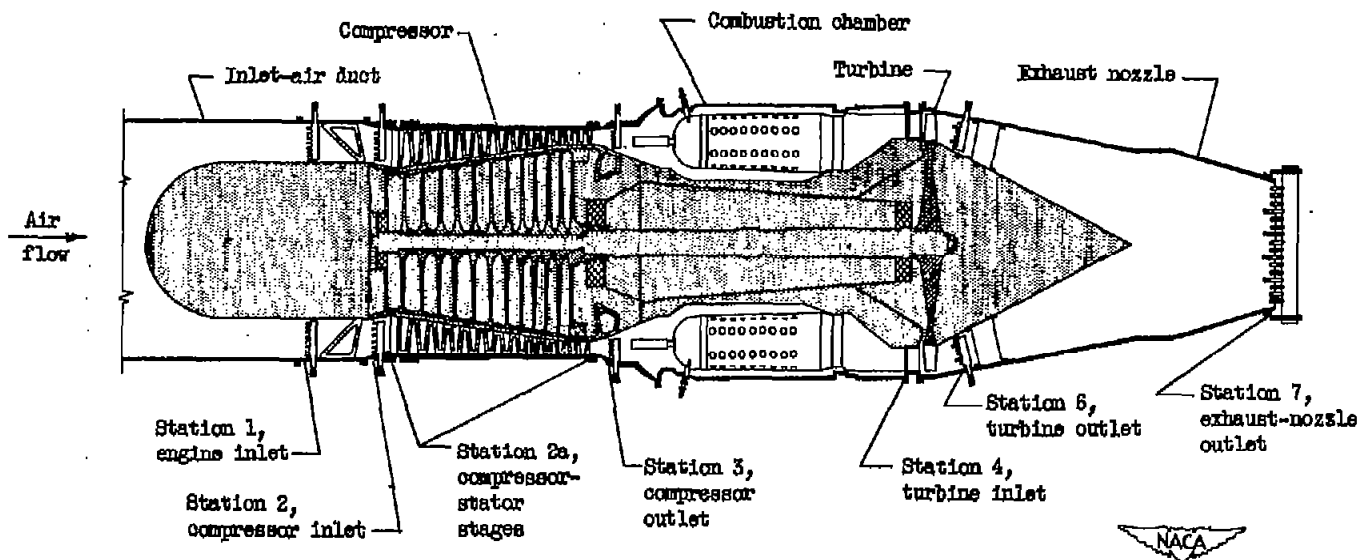


Figure 1. - Installation of turbojet engine in altitude wind tunnel.



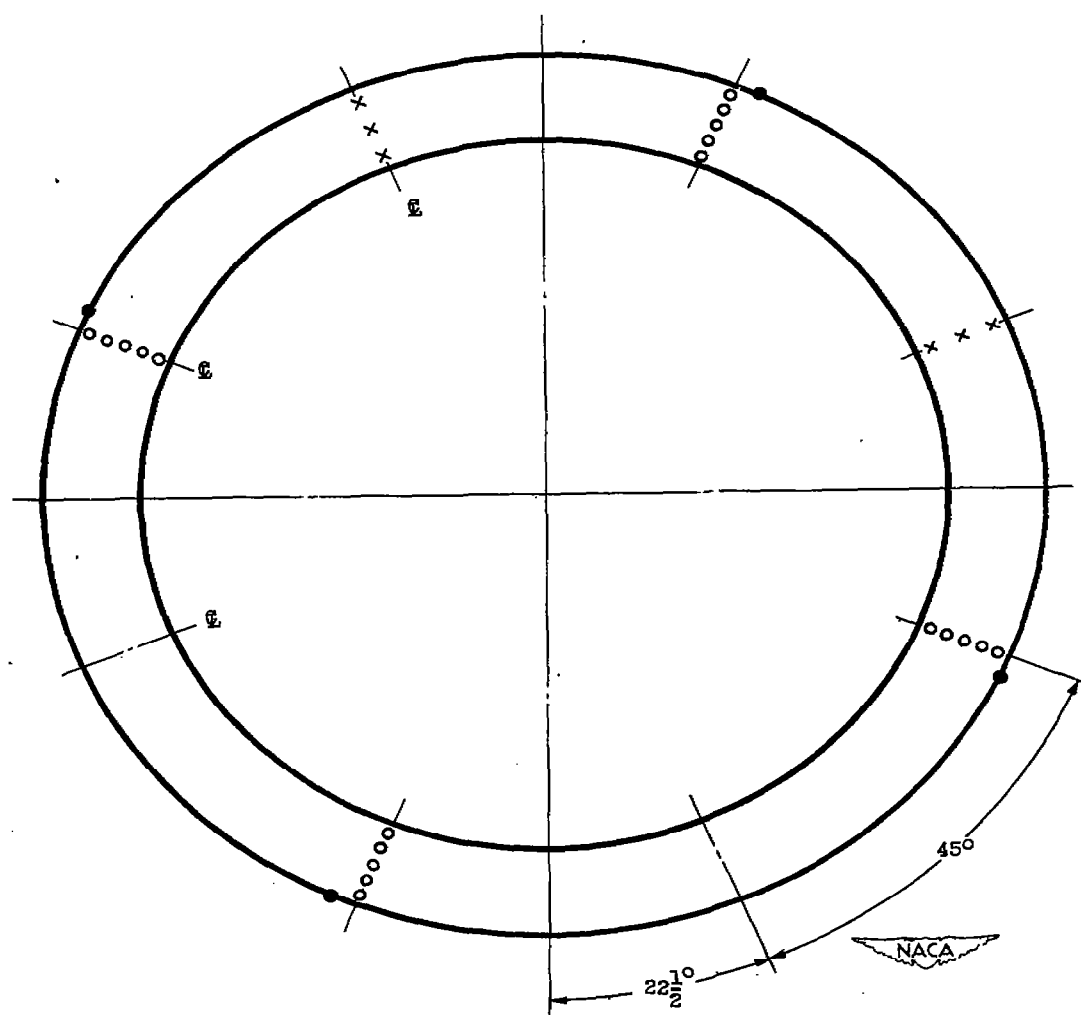




Station	Total-pressure tubes	Static-pressure tubes	Wall static-pressure orifices	Thermo-couples
1	40	4	0	8
2	24	0	4	0
2a	0	0	13	0
3	20	0	4	6
4	5	0	0	0
6	30	0	2	24
7	18	5	4	14

Figure 2. - Cross section of turbojet-engine installation showing sections at which instrumentation was installed.

- Total-pressure tube
- Static-pressure wall orifice
- × Thermocouple
- ⊕ Combustion-chamber center line



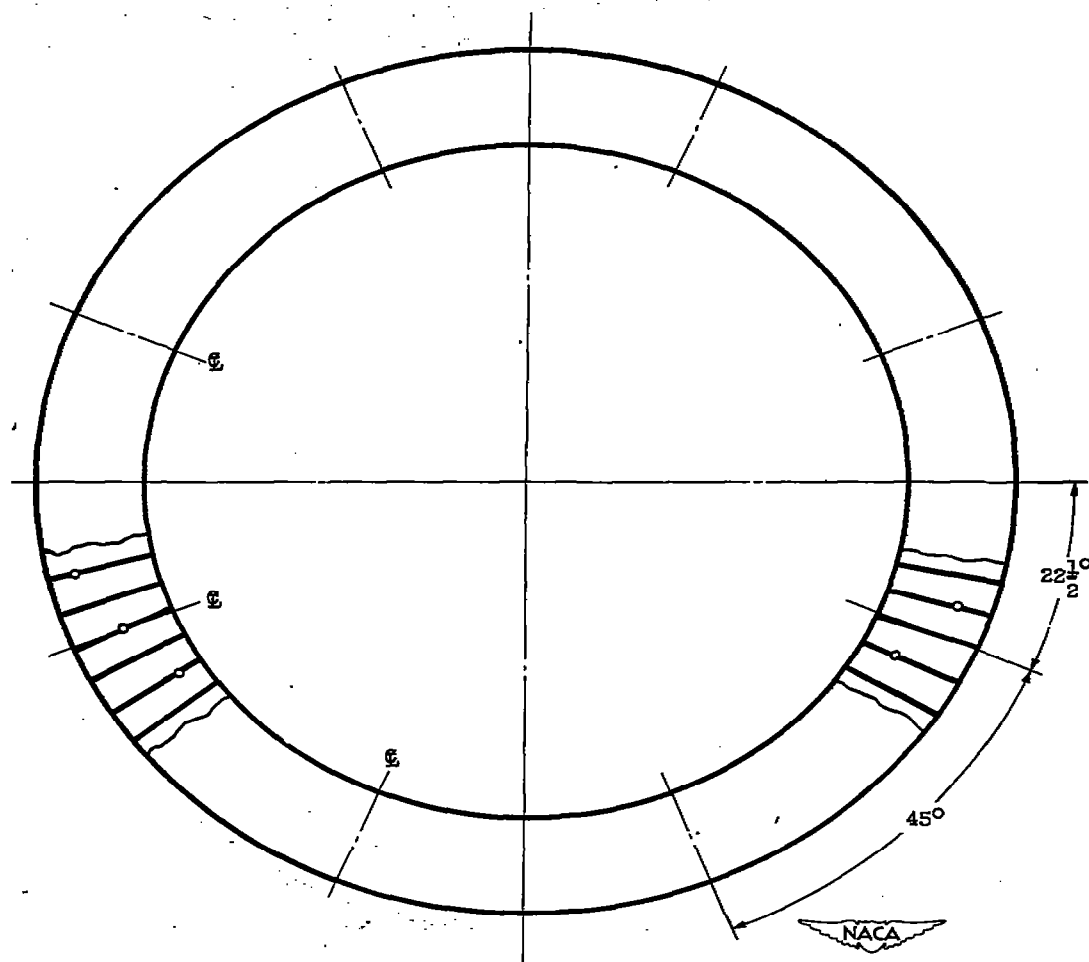
(a) Compressor outlet, station 3;  $3\frac{1}{4}$  inches behind trailing edge of outlet guide vanes.

Figure 3. - Instrumentation of turbojet engine. Viewed from upstream.

1218

462-1767

- Total-pressure tube  
 ② Combustion-chamber center line



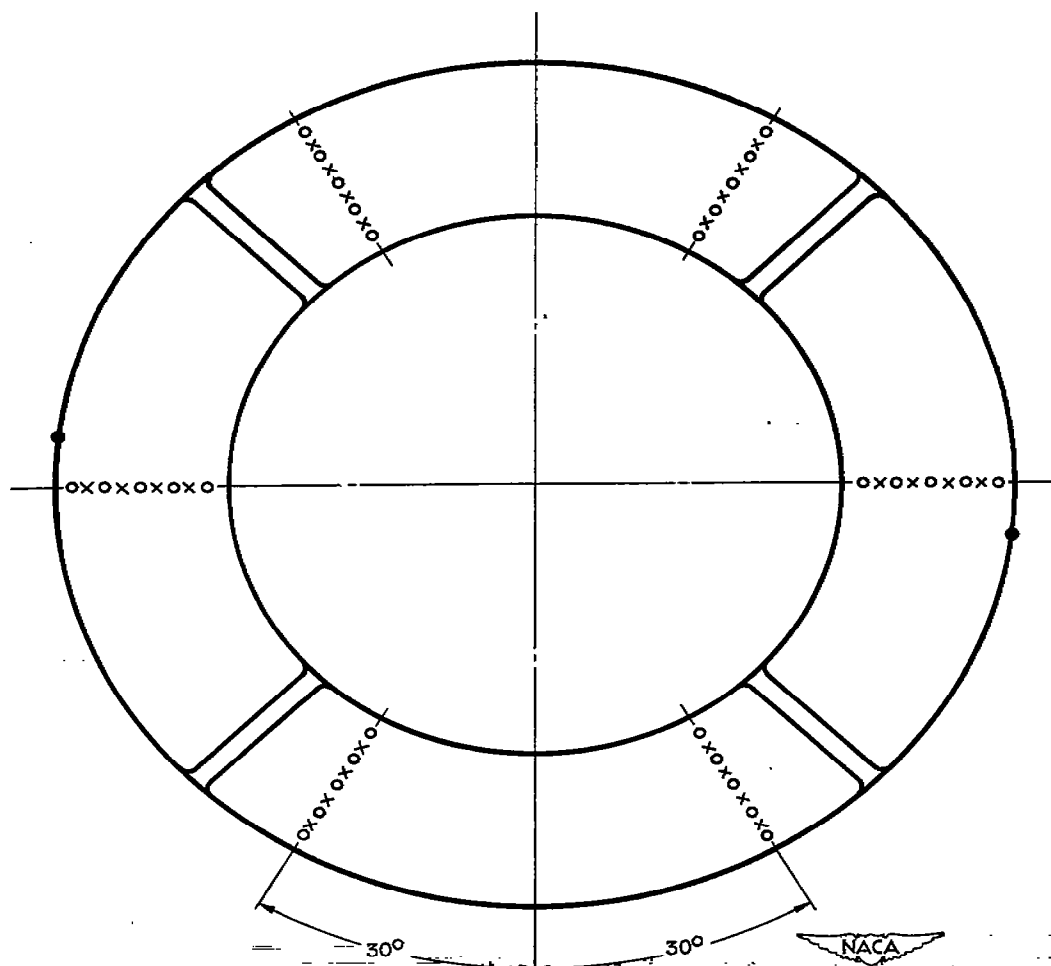
(b) Turbine inlet, station 4; in plane of leading edge of turbine-stator blades.

Figure 3. - Continued. Instrumentation of turbojet engine. Viewed from upstream.

1218

462-1768

- Total-pressure tube
- Static-pressure wall orifice
- × Thermocouple



(c) Turbine outlet, station 6; 10 $\frac{1}{2}$  inches downstream of turbine flange.

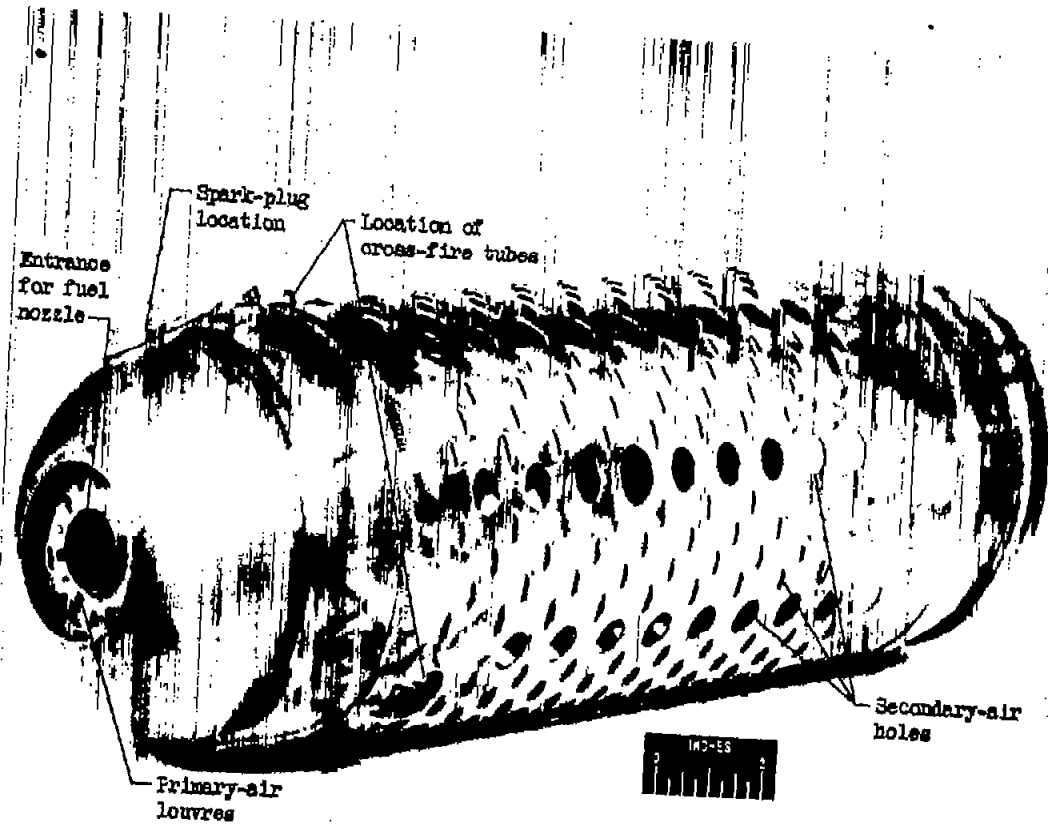
Figure 3. - Continued. Instrumentation of turbojet engine. Viewed from upstream.

1218

462-1169







C-23526  
6-1-49

Figure 4. - Three-quarter front view of combustion-chamber liner.





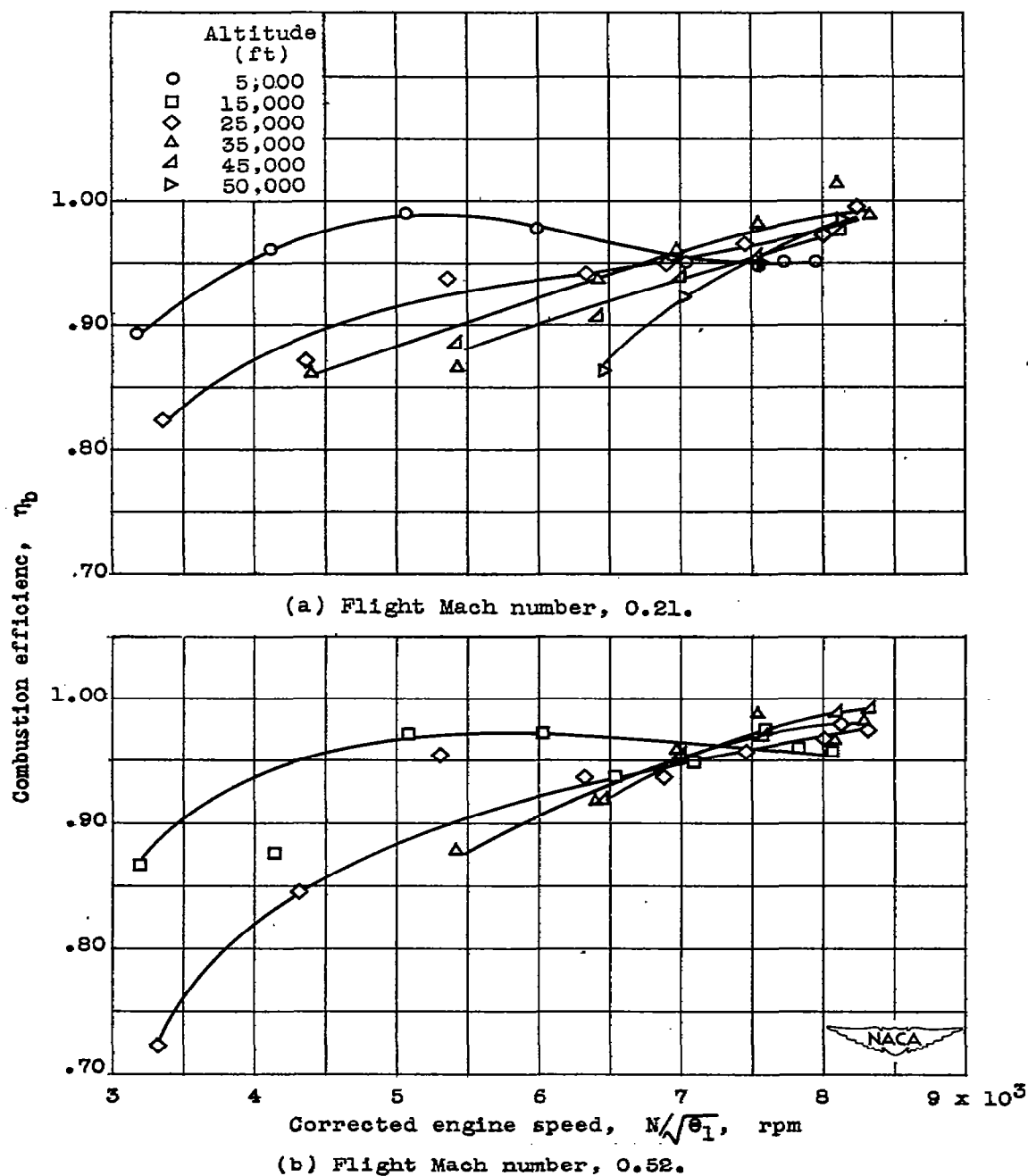


Figure 5. - Effect of corrected engine speed and altitude on combustion efficiency of engine with standard exhaust nozzle at flight Mach numbers of 0.21 and 0.52.

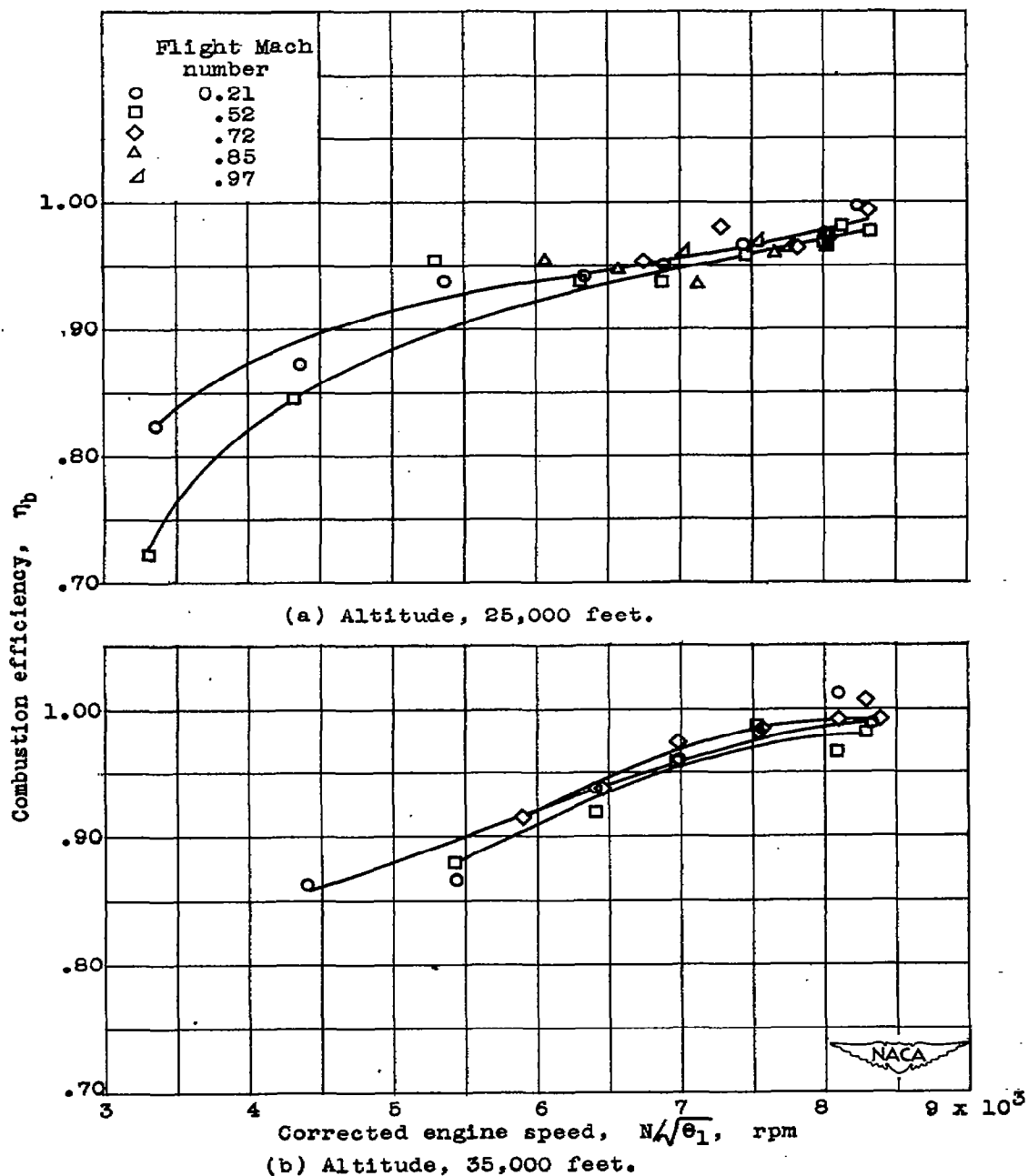


Figure 6. - Effect of corrected engine speed and flight Mach number on combustion efficiency of engine with standard exhaust nozzle at altitudes of 25,000 and 35,000 feet.

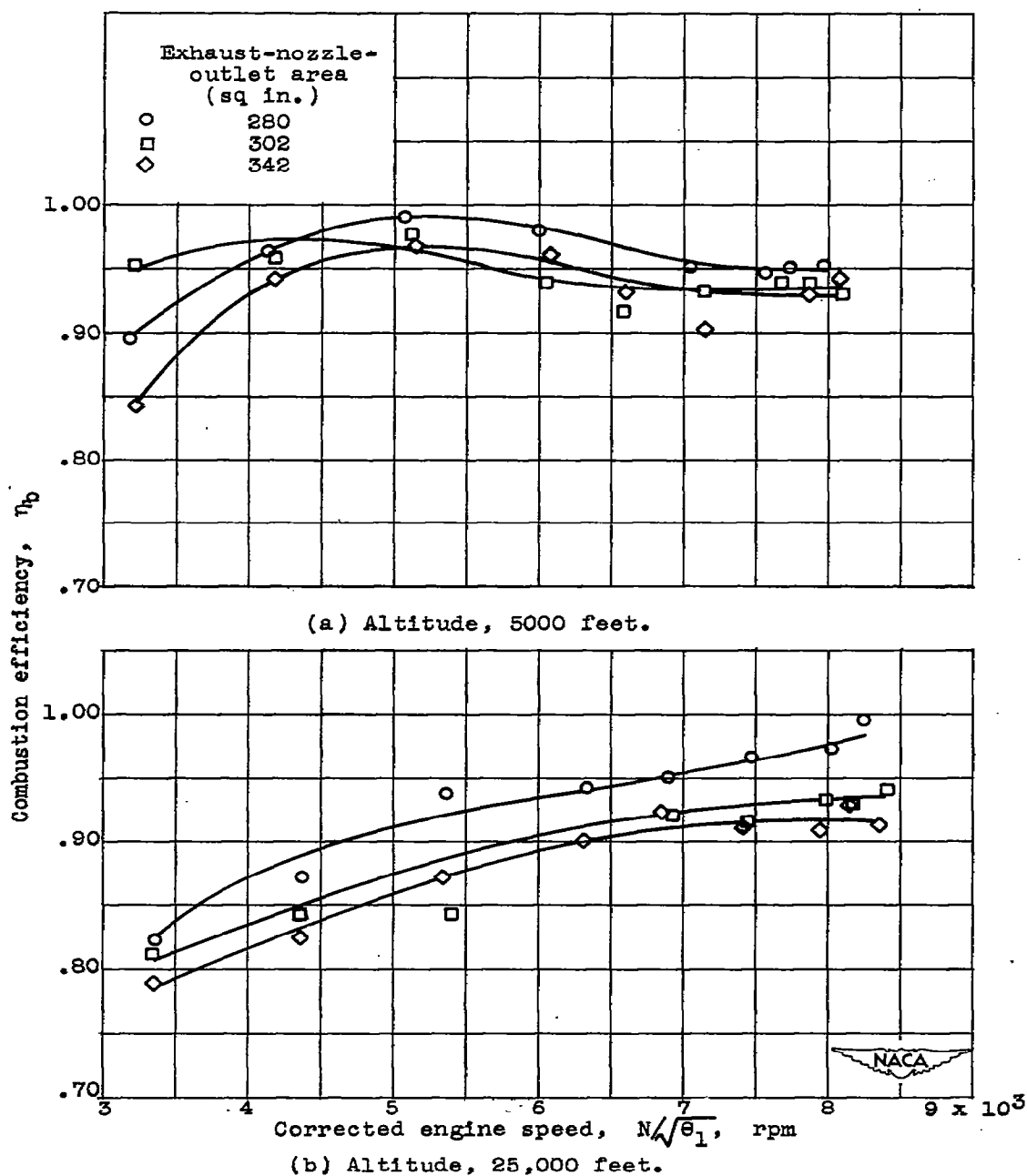
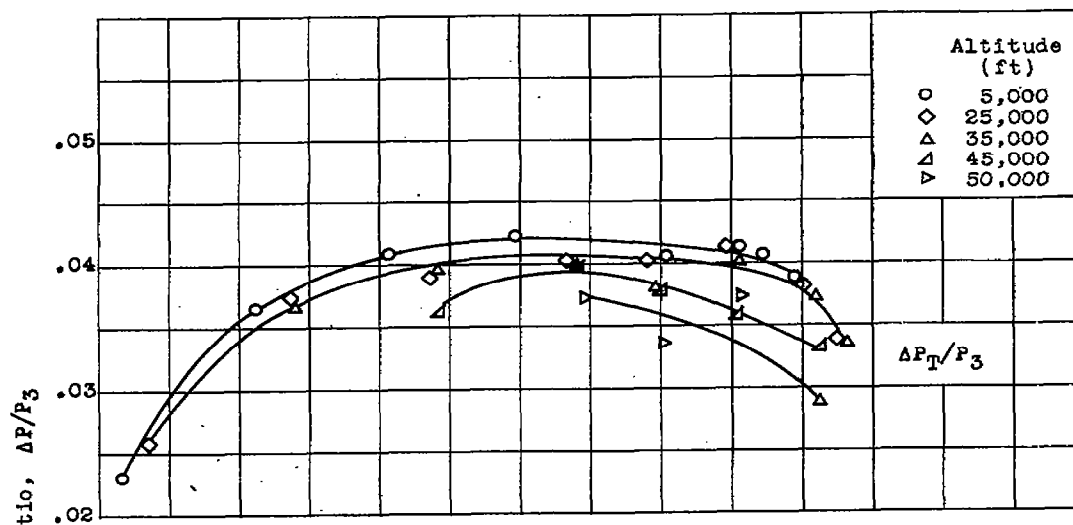
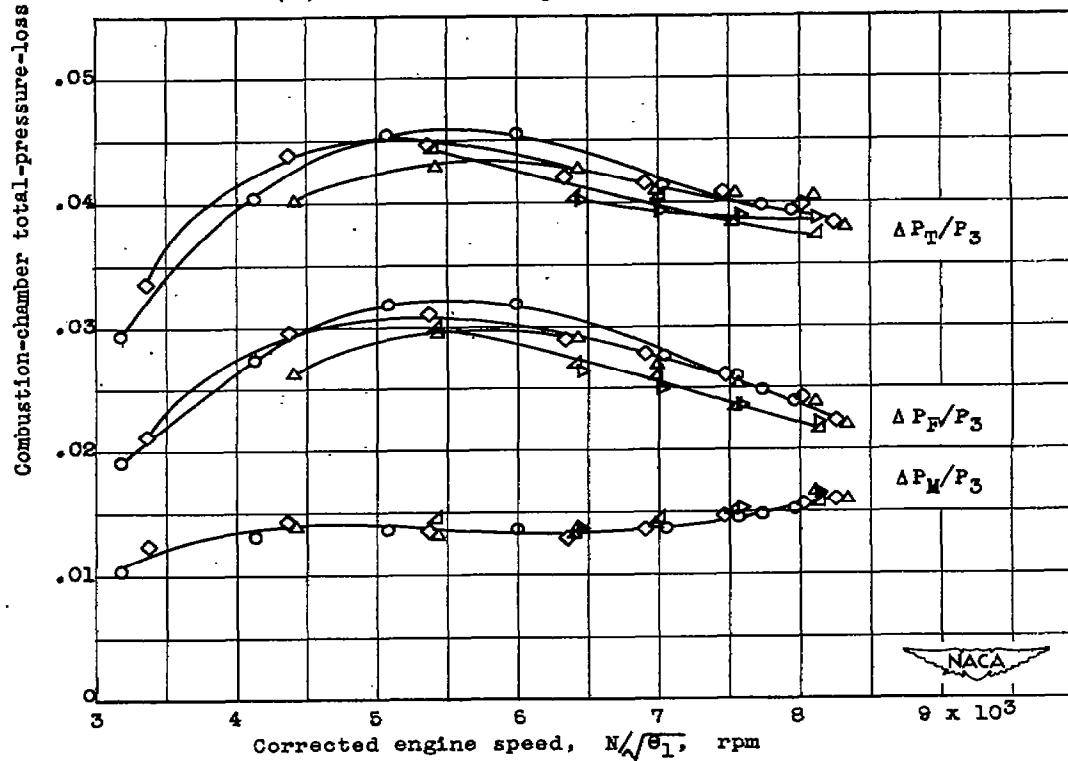


Figure 7. - Effect of corrected engine speed and exhaust-nozzle-outlet area on combustion efficiency of engine at altitudes of 5000 and 25,000 feet and flight Mach number of 0.21.

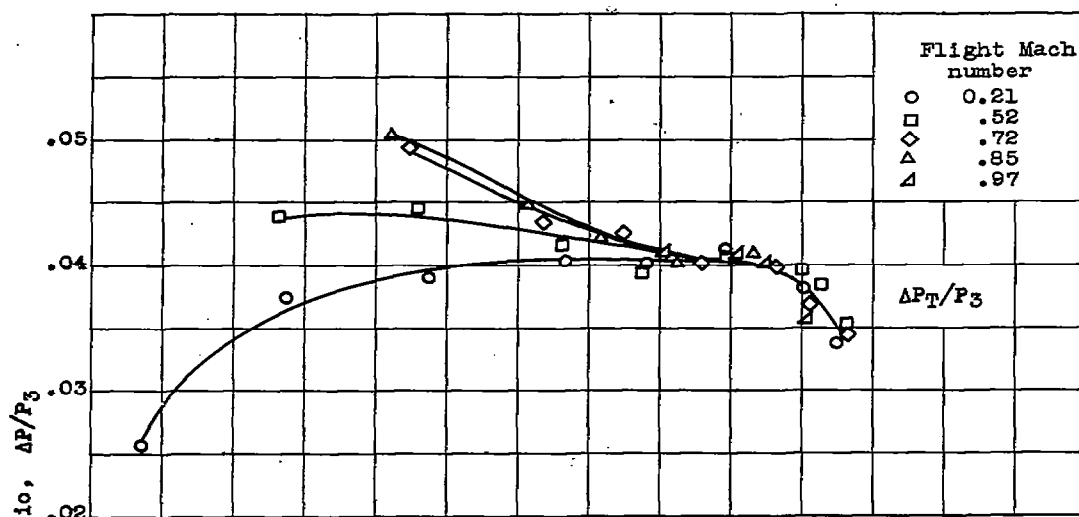


(a) Measured total-pressure-loss ratio.

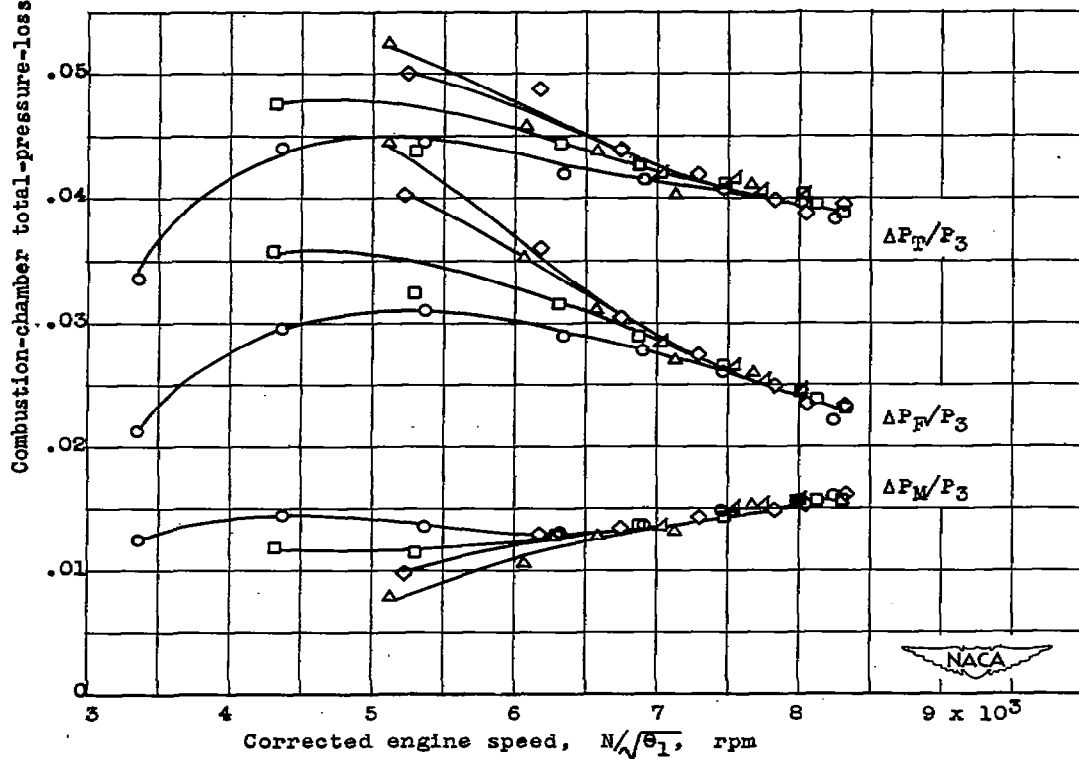


(b) Calculated total-pressure-loss ratio.

Figure 8. - Effect of corrected engine speed and altitude on measured and calculated total-pressure-loss ratios through combustion chamber of engine with standard exhaust nozzle at flight Mach number of 0.21.



(a) Measured total-pressure-loss ratio.



(b) Calculated total-pressure-loss ratio.

Figure 9. - Effect of corrected engine speed and flight Mach number on measured and calculated total-pressure-loss ratios through combustion chamber of engine with standard exhaust nozzle at altitude of 25,000 feet.

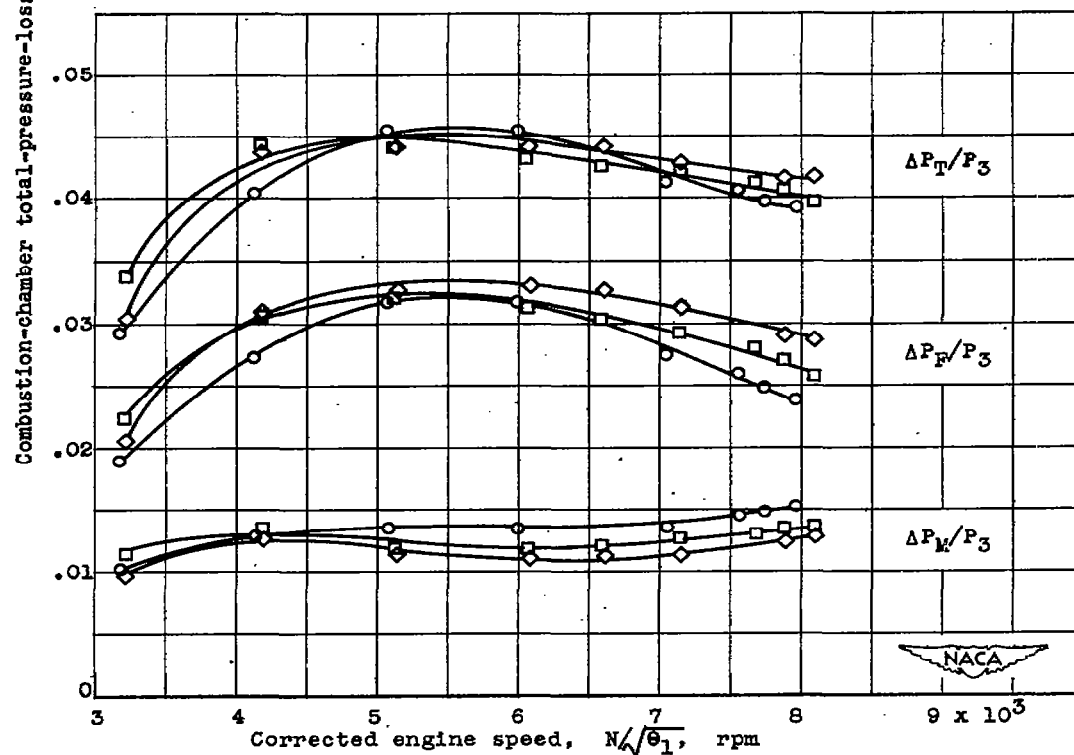
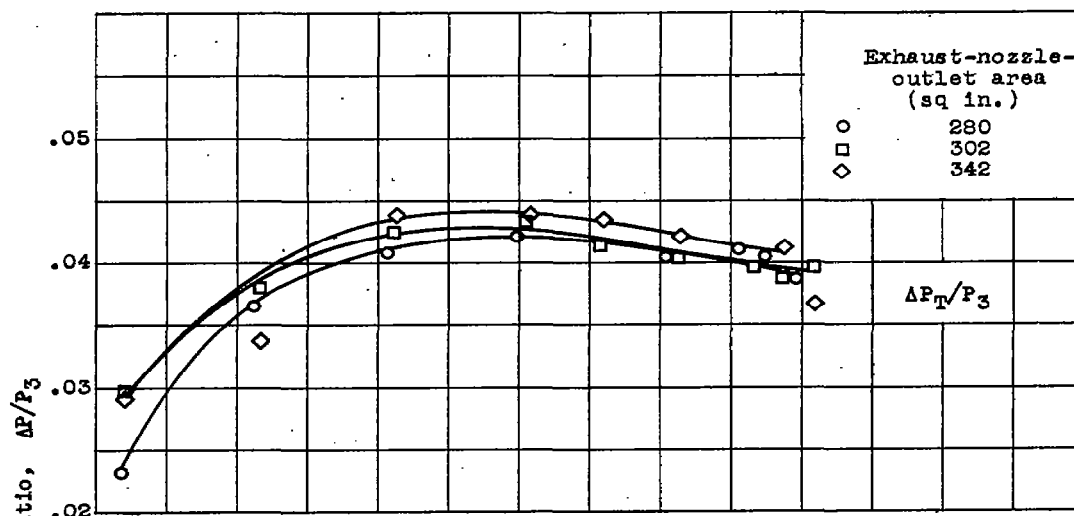
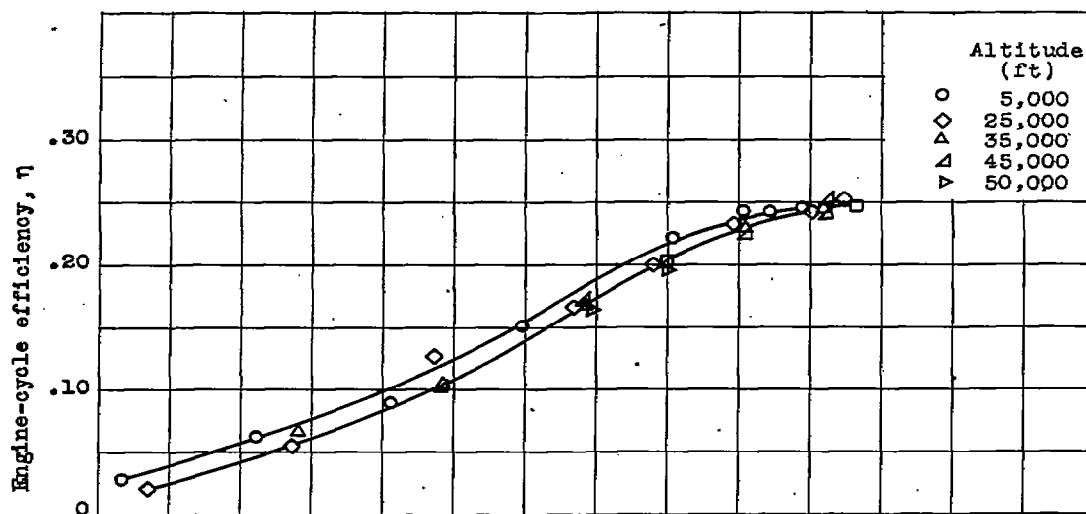
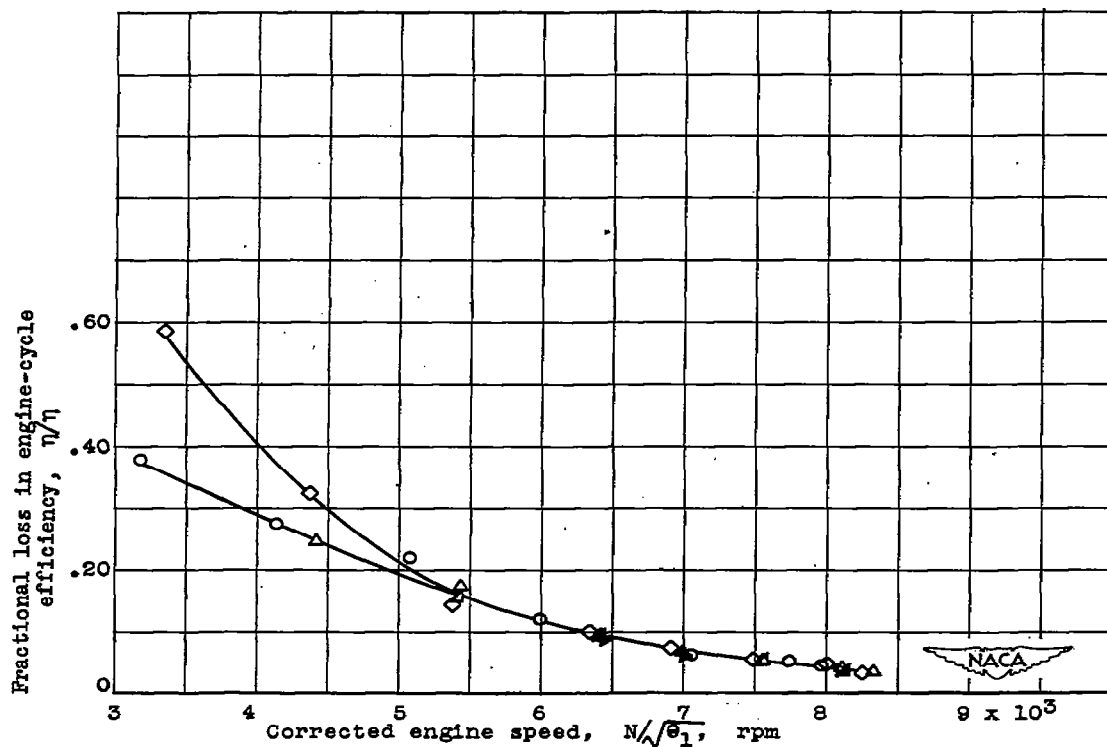


Figure 10. - Effect of corrected engine speed and exhaust-nozzle-outlet area on measured and calculated total-pressure-loss ratios through combustion chamber of engine at altitude of 5000 feet and flight Mach number of 0.21.



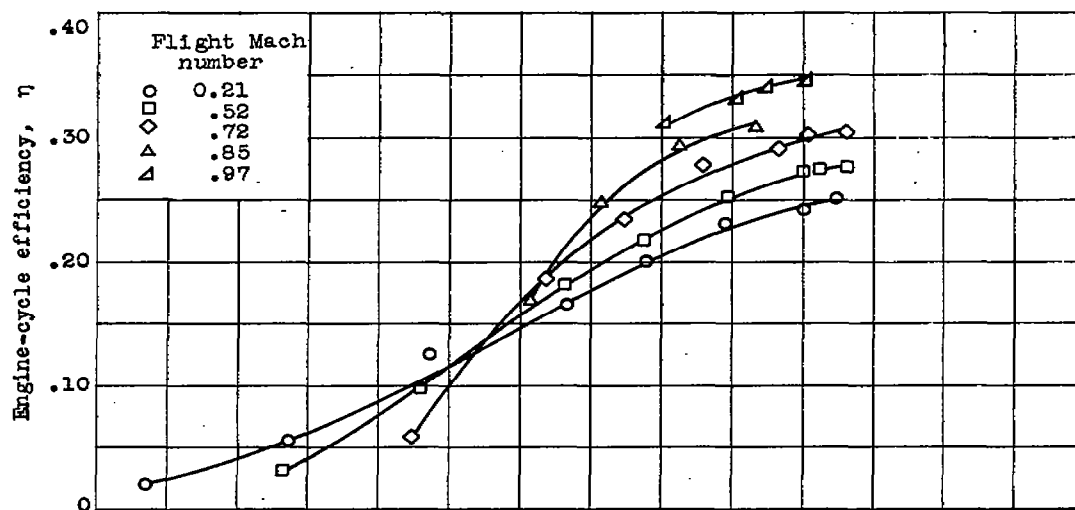
(a) Engine-cycle efficiency.



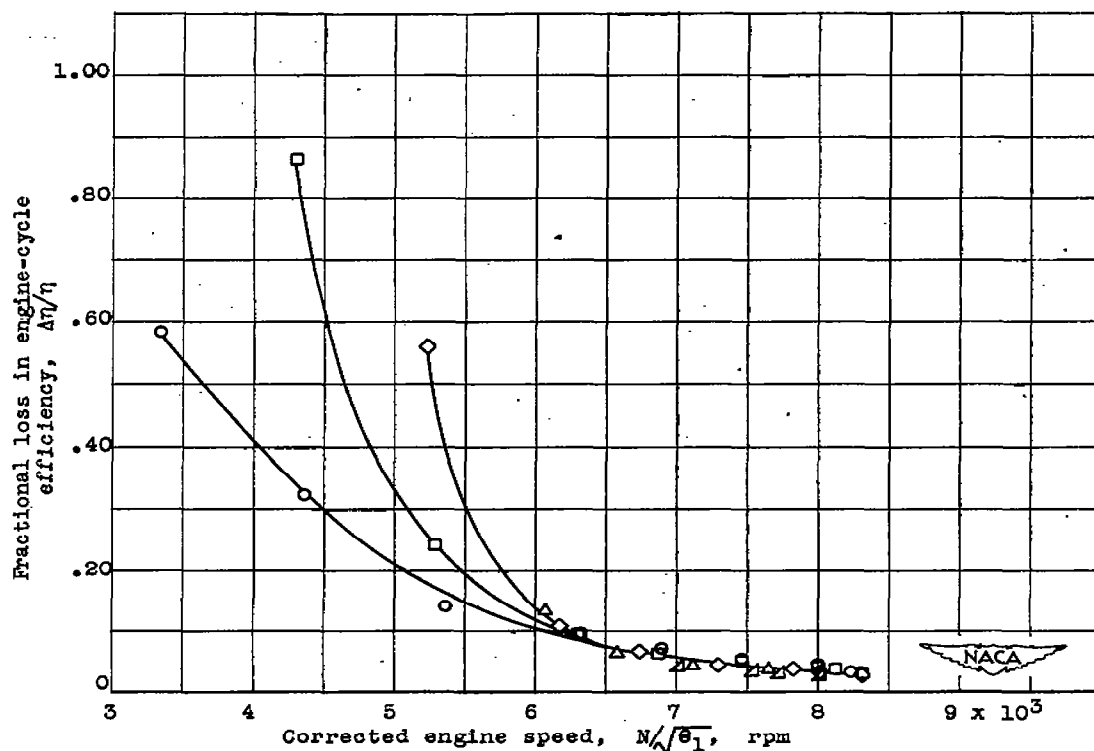
(b) Fractional loss in engine-cycle efficiency.

Figure 11. - Effect of corrected engine speed and altitude on engine-cycle efficiency and fractional loss in engine-cycle efficiency with standard exhaust nozzle at flight Mach number of 0.21.



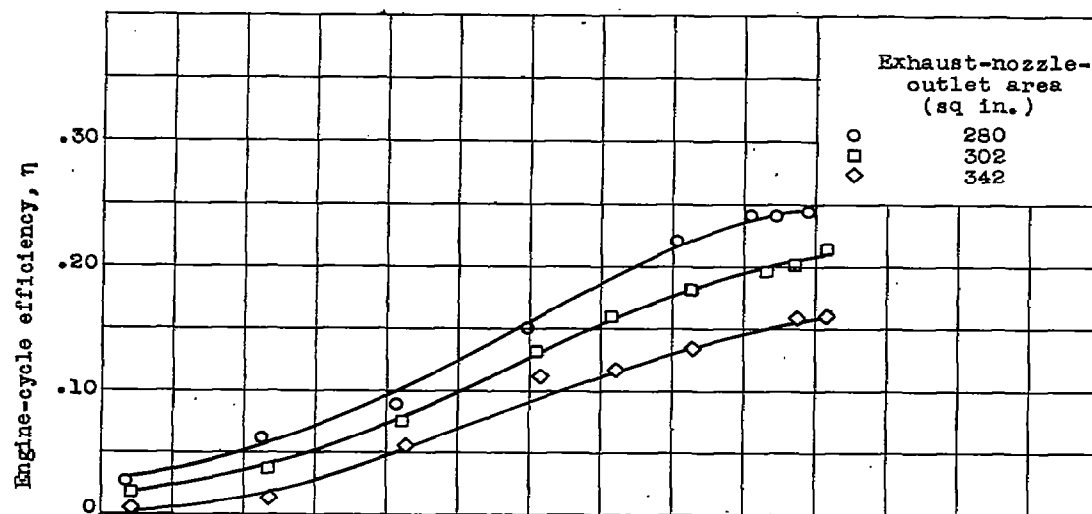


(a) Engine-cycle efficiency.

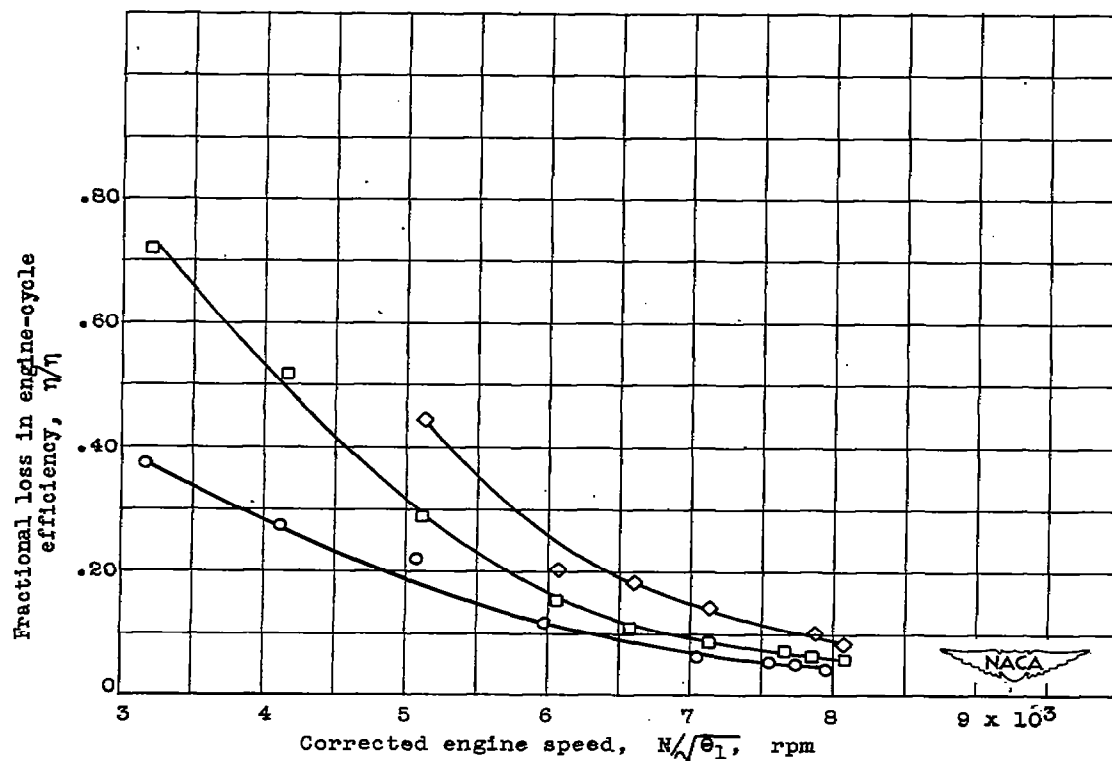


(b) Fractional loss in engine-cycle efficiency.

Figure 12. - Effect of corrected engine speed and flight Mach number on engine-cycle efficiency and fractional loss in engine-cycle efficiency with standard exhaust nozzle at altitude of 25,000 feet.



(a) Engine-cycle efficiency.



(b) Fractional loss in engine-cycle efficiency.

Figure 13. - Effect of corrected engine speed and exhaust-nozzle-outlet area on engine-cycle efficiency and fractional loss in engine-cycle efficiency at altitude of 5000 feet and flight Mach number of 0.21.